C 7 the combination of biological stain/photosensitizer and a spectrometer means of analyzing the stain *in situ*.--

IN THE CLAIMS:

Please cancel claims 12, 13 and 17-19 and amend claims 1, 5 and 7-11 as outlined in Appendix 1. A copy of the amended claims showing the changes made is included herein as Appendix 1. A copy of the entire set of pending claims after entry of this amendment is provided herein as Appendix 2.

REMARKS

Entry of the above amendments and reconsideration of the application are respectfully requested. After entry of the amendments, claims 1, 5, and 7-11 are pending. Claims 12, 13 and 17-19 have been cancelled and claim 1 has been amended to indicate that the degree of the metachromatic shift of the dye from the reflected light spectrum of the stained tissue or cells is compared with the degree of the metachromatic shift of the dye obtained from a library of previously obtained reflected light spectra of similarly stained tissue or cells. Such an amendment is supported, for example, on page 8, lines 9-16, and page 22, lines 1-5, and is not believed to add new matter.

Claim 1 has also been amended to indicate that the method is for diagnosing dysplasia, pre-cancer and cancer and that the dyes utilized are methylene blue and toluidine blue O. The former amendment regarding the disease state that is diagnosed is supported, for example, on page 8, lines 14-16. The latter amendment regarding the dyes utilized is supported, for example, on page 8, line 29 to page 9, line 2; page 22, line 29 to page 23, line 1; and page 20, lines 5-8. Claims 5 and 7-11 have been amended to correct various typographical errors or to more precisely claim the invention. Additionally, the specification has been amended to correct various typographical errors.

The specification has been objected to as it is asserted certain terms are misspelled. Additionally, various claims stand rejected under 35 U.S.C. § 112, first and

second paragraphs and under 35 U.S.C. §102(b) over cited art. In light of the discussion below, it is believed that the above objection and rejections of record have been overcome and that all pending claims are in condition for allowance. Action toward this end is respectfully solicited.

Applicants and their attorneys would like to thank Examiners Rawlings and Wortman for the courtesies they extended during the interview on January 29, 2002. Prior to discussion of the objection and rejections of record, applicants would like to discuss exemplary experimental data (reported in Exhibit A) obtained according to the methods of the invention that was discussed with the Examiners during the aforementioned interview. The data in Exhibit A submitted herewith were obtained by Dr. Patrick Walsh at the University of Colorado Health Sciences Center (Anschutz Cancer Center) according to the methods described in the above-referenced specification. The data collectively exemplify how the methods of the present invention have been practiced with toluidine blue O and methylene blue and applied to diagnose, for example, cancer in variety of tissue samples.

EXHIBIT A

A variety of tissue samples listed in Table 1 on page 17 was stained with methylene blue and utilized to generate a library of spectra so that the pathology of test tissue samples could be easily diagnosed according to the methods of the present invention. The stained tissue samples were analyzed with a multispectral image system under software control as described in Exhibit A, and a red-green-blue (RGB) composite image and a region of interest (ROI) graph were generated for each sample. The ROI graphs were analyzed to determine the extent of the metachromatic shift of the dye utilized. Such information from a subset of the samples in Table 1 was then utilized to generate various metachromatic indices as discussed on page 15 of Exhibit A and to subsequently diagnose the pathology of a test tissue sample. The tissue samples were subsequently diagnosed by conventional histological techniques (e.g., cryostat, fixation and automated staining with either toluidine blue O or haematoxylin-eosin).

As one example of practicing the methods of the present invention, an RGB image and ROI graph were obtained by analysis of a freshly-excised methylene blue-

stained nasal tissue sample (01.025), subsequently diagnosed as normal by conventional histological techniques as described above and in Exhibit A, and are shown on pages 4 and 5, respectively, of Exhibit A. Analysis of the ROI graph revealed only very slight metachromasia.

As a further example, the RGB image and ROI graph obtained by analysis of a methylene blue-stained tissue sample (01.027) and diagnosed as basal cell carcinoma by the conventional technique described above are shown on pages 10 and 11, respectively. The red region of interest shown in the ROI graph clearly displayed a significant metachromatic shift toward wavelengths shorter than 670 nm.

In addition to tissue sample 01.025 and 01.027, tissue samples 01.003-01.024 and 01.026 listed in Table 1 of Exhibit A were similarly stained with methylene blue and the extent of the metachromatic shift of the dye was obtained from the reflected light spectra as described in the specification and Exhibit A. The pathology of these samples was also confirmed by the conventional technique described above, in the specification and in Exhibit A, and the spectral features of the reflectance spectra of the above-mentioned samples were noted.

For example, for those samples displaying a positive metachromatic spectral signature and which correlate with subsequent histopathological diagnosis, it was found that the principal absorption spectrum (for methylene blue) centers near 665 to 670 nm and displays a metachromatic shift with an increase in absorption toward the yellow/green wavelengths. By inspection, principal noted features are "shoulders" centered near 600 nm and 640 nm which often exceed the peak absorption intensity at 670 nm. These features correspond to known spectral shifts of methylene blue. These spectral features are metachromatic indices [(MI); including MI Class 1, MI Class 2, MI 01, MI 45 and negative MI (MI 0)] as described, for example, at page 15 of Exhibit A.

This library of spectral data was then used to diagnose the pathology of tissue samples 01.032-01.040 according to the methods of the present invention. The pathology of samples 01.032-01.040 was also subsequently confirmed by the conventional histological technique described above.

As seen in Table 1, the diagnosis of the pathology of tissue samples 01.032, 01.038 and 01.040 as non-cancerous and tissue samples 01.033-01.37 and 01.039 as

cancerous according to the methods of the present invention agreed with the diagnosis obtained by the conventional technique described above.

In the aforementioned samples studied, no residual clotted blood was present in the samples. In order to evaluate the potential interference of hemoglobin in samples having residual clotted blood with observation of the metachromatic properties of methylene blue staining, a freshly-excised tissue sample having such clotted blood and whose pathology was diagnosed as a basal cell carcinoma lesion was stained with methylene blue and analyzed as described above and in Exhibit A. As seen in the ROI graph on page 9, although a hemoglobin spectra is observed, the influence of any absorption due to heme in the range of 630-690 nm, which is the principal region of methylene blue metachromasia, is minimal.

Additionally, similar diagnoses were made when practicing the methods of the present invention with toluidine blue O. An exemplary RGB image and ROI graph of toluidine blue O-stained scalp tissue sample is shown on page 21 of Exhibit A. It was determined that the MI 0 spectral feature identified for the methylene blue stain could also be utilized to diagnose samples stained with toluidine blue O.

The results of the study with respect to toluidine blue O are shown in Table 2 on page 22 of Exhibit A. As seen in Table 2, tissues determined to be cancerous by a conventional technique were correctly identified as cancerous tissue samples when practicing the method according to the present invention.

It is noted that Exhibit A further includes a variety of metaspectral image maps of the methylene blue-stained samples on pages 12, 13 19 and 20 and toluidine blue O samples on page 23 to indicate the location of the abnormal tissue in the sample.

In conclusion, the above-discussed data show, among other things and by analyzing a variety of tissue samples, that cancerous tissue may be distinguished from non-cancerous tissue when stained with a metachromatic dye by obtaining a reflected light spectrum of the stained tissue and comparing the degree of the metachromatic shift of the dye from the reflected light spectrum of the stained tissue with the degree of the metachromatic shift of the dye from a library of previously obtained spectra of similarly stained tissue according to the methods of the present invention without undue experimentation.

Additionally, the results in Exhibit A further show that hemoglobin present in samples having residual clotted blood does not interfere with the practice of the diagnostic methods of the present invention. Accurate results are thus obtained in the presence or absence of residual clotted blood, the advantages of which will be appreciated by those of skill in the art.

Objection to the Specification

It is asserted in the Action that the terms "metaplasic" and "dysplasic" are misspellings of the terms "metaplastic" and "dysplastic". Applicants thank the Examiner for noting these typographical errors. Applicants have amended the specification to correct these and other typographical errors. Entry of these amendments and withdrawal of the objection to the specification are respectfully requested.

Rejection of claims 1, 5, and 7-12 under 35 U.S.C. § 112, first paragraph

Claims 1, 5 and 7-12 stand rejected under 35 U.S.C. § 112, first paragraph. It is asserted that (1) the recited method does not distinguish cells or tissues to which the method can be applied from those to which it can not be applied; (2) there are no working examples in the specification to provide guidance; (3) the specification does not teach use of all thiazine dyes and each dye would have different staining properties; and (4) the specification does not teach use of the method to diagnose any disease state. The Action concludes that one of skill in the art "would not accept the assertion that the method can be used to the breadth of the scope of the claims with a reasonable expectation of success based only upon the instant disclosure." This ground of rejection is respectfully traversed. Applicants note that claim 12 has been cancelled and therefore the rejection as to this claim is now moot. Applicants assert that the specification provides sufficient guidance to the skilled artisan to practice the claimed invention as will be discussed below and as evidenced by the experiments that were conducted according to the methods outlined in the specification without undue experimentation as discussed above and in Exhibit A submitted herewith.

The present invention relates to a method for diagnosing a disease state *in situ* in biological tissue or cells of a living organism that includes utilization of spectroscopic methods to analyze the metachromatic properties of various dyes in abnormal (e.g., dysplastic, pre-cancerous and cancerous) and normal cells. The inventors of the present invention have discovered that the extent of the metachromatic shift observed in a dye from stained tissue or cells can be used to differentiate, for example, the aforementioned abnormal cells and/or tissues from normal cells and/or tissues. According to one embodiment of the methods described in the application, the metachromatic shift of a dye observed in the reflected light spectrum from a dye-stained test sample is compared to the metachromatic shift of the dye from a library of previously obtained spectra of similarly stained tissue or cells wherein the diagnosis of the disease state of the reference cells or tissue upon which the previously obtained spectra are based was confirmed by conventional histochemical methods. Thus, quicker, more precise diagnoses may be made according to the present method compared to existing methods.

Turning now to the rejections of record, and specifically that the recited method does not distinguish cells or tissues to which the method can be applied from those cells or tissue to which it can not be applied, applicants assert the present specification teaches that the methods of the invention can be practiced to diagnose disease states in a wide variety of cells or tissues. Applicants further assert that the specification is replete with examples of cells and/or tissue types, such as abnormal or otherwise cancerous cells and/or tissues, that may be diagnosed according to the methods of the present invention, as will be appreciated by those of skill in the art who have read and understood the specification.

For example, a wide variety of abnormal or otherwise cancerous cells can be stained by thiazine dyes, such as methylene blue and toluidine blue O. On page 4, lines 10-14, of the application, for example, it is mentioned that toluidine blue O has been utilized for staining oral squamous cell carcinomas, basal cell carcinomas of the skin, and cervical carcinomas. Additionally, it is discussed on page 5, lines 4-5 and 8-9, of the application that methylene blue has been used to stain intestinal metaplasia in Barrett's esophagus and bladder cancers, respectively.

In addition to this guidance in the present specification, one skilled in the art would also be familiar with other abnormal cells and/or tissues that may be stained and whose pathology may be consequently diagnosed utilizing the dyes described in the specification. For example, sarcoma 180 cells, Gardner lymphoma cells and mammary adenocarcinoma cells are able to take up various phenothiazine dyes in photochemical inactivation studies as discussed, for example, in Tuite, E.M. and Kelly, J.M., *Photochem. Photobiol. B:Biol*, 21:103-124 (1993) (Exhibit B). As a further example, pancreatic tumor cells and parathyroid adenomas can be stained with methylene blue, as discussed, for example, in Fedorak, I.J. et al. *Surgery* 113(3):242-249 (1993) (Exhibit C) and Meekin, G.K. *The Laryngoscope* 108:772-773 (1998) (Exhibit D), respectively.

Additionally, thiazine dyes such as, for example, methylene blue have been found to improve the ability of other anticancer drugs to penetrate into tissue and "to diffuse through the epidermis and enter channel networks draining the dermis" in, for example, breast cancer, melanoma, ovarian cancer and lung cancer as described in Morgan, L.R. et al. *Biorg. & Med. Chem. Lett.* 2193-2195 (2001) (Exhibit E). Similarly, methylene blue has been shown to increase the sensitivity of multidrug resistant cells to the dye and its photodynamic action as discussed in Trindade, G.S. et al. *Cancer Letters* 151:161-167 (2000) (Exhibit F). Therefore, lipophilic cationic dyes, such as the phenothiazine dyes and including methylene blue and toluidine O, have been shown to, and would be expected to, stain a wide variety of tissue and/or cell types.

Moreover, if there were some doubt as to whether a specific cell/tissue type could take up a stain described in the specification, such as methylene blue or toluidine blue O, a determination could be made as to the ability of the cell/tissue to take up the stain utilizing standard procedures known to the skilled artisan. Such experimentation would not be undue. As the specification is replete with examples of cells and/or tissues that may be diagnosed in the invention, and one skilled in the art is familiar with such tissues/cells as well as a wide variety of other cells/tissues, one skilled in the art would be able to practice the invention to the full breadth as claimed without undue experimentation.

Turning now to the rejection asserting that there are no working examples in the specification to provide guidance, it is well-settled that a specification can be enabling without any working examples. *In re Borkowski*, 164 U.S.P.Q. 642, 645 (C.C.P.A. 1970). Applicants assert the specification is sufficiently enabling as drafted with respect to the pending claims as further described herein. The Examiner is also invited to review the data, obtained following the guidance provided in the application and without undue experimentation, presented in Exhibit A and discussed above.

Turning now to the rejection asserting that the specification does not teach use of all thiazine dyes and each dye would have different staining properties, applicants assert there is no support offered in the Action for the contention that related thiazine compounds, the properties of which are well-characterized and known in the art, would be expected not to function when used according to the teachings of the present invention, and applicants are unaware of any basis for such a contention. To the contrary, the metachromatic properties of thiazine compounds observed by applicants and described in the specification are believed to apply to the members of this class of compounds, and the person of ordinary skill in the art who reads and understands the present specification could utilize other thiazine dyes with the application of normal, and not undue, experimentation.

Nevertheless, in a sincere attempt to advance prosecution, and without prejudice to or disclaimer of the broader application of the invention, applicants have amended claim 1 to recite that the dyes are selected from the group consisting of methylene blue and toluidine blue O. As mentioned above, these dyes are known to stain a wide variety of cells and/or tissues, including various abnormal cells and/or tissues.

Turning now to the rejection relating to the assertion that the specification does not teach use of the method to diagnose any disease state, although applicants believe the specification provides support for practicing the claimed method to diagnose a wide variety of disease states, applicants have amended claim 1 in a sincere attempt to advance prosecution to recite that the claimed method is utilized to diagnose dysplasia, pre-cancer or cancer, without disclaimer of or prejudice to the broader application of the invention which applicants have taught those of skill in the art in the present specification, and is more than sufficiently supported by the specification.

In light of the above discussion, it is believed that the breadth of the pending claims is fully supported by the specification. Withdrawal of the rejection of claims 1, 5 and 7-11 under 35 U.S.C. § 112, first paragraph is respectfully requested. As claim 12 has been cancelled, withdrawal of the rejection of claim 12 under 35 U.S.C. § 112, first paragraph is also respectfully requested.

Rejection of claims 13 and 17-19 under 35 U.S.C. § 112, first paragraph

As claims 13 and 17-19 have been cancelled, the rejection as to these claims is now moot. Withdrawal of the rejection of claims 13 and 17-19 under 35 U.S.C. § 112, first paragraph is respectfully requested.

Rejection of claims 1, 5, and 7-12 under 35 U.S.C. § 112, second paragraph

It is asserted that claims 1, 5, 7-13 and 17-19 are indefinite for the reasons that follow. This ground of rejection is respectfully traversed. As claims 12, 13 and 17-19 have been cancelled, the rejection as to these claims is now moot.

It is asserted that claims 1, 5 and 7-12 are vague and indefinite due to the recitation of the phrase "comparing the reflected spectrum" as it is asserted it is not clear how the spectra are to be compared or what aspect or characteristic of the spectrum is to be compared with the library of previously obtained spectra. Applicants assert that the pending claims would be sufficiently definite to the skilled artisan with respect to the recitation of "comparing the reflected spectrum."

The specification teaches on page 22, lines 1-3, for example, that in one form of the invention the metachromatic shift of the stain utilized may be compared between two or more specific wavelengths. Although applicants do not believe amendment of claim 1 to include such a limitation is required to obviate this rejection, claim 1 has been amended to delineate that the degree of the metachromatic shift of the dye from the reflected light spectrum of the stained tissue or cells is compared with the degree of the metachromatic shift of the dye from a library of previously obtained reflected light

spectra of similarly stained tissue or cells. Thus, one skilled in the art would be reasonably apprised of the metes and bounds of the invention.

It is further asserted in the Action that, with respect to claims 1 and 12 which recite the phrase "with a library of previously obtained spectra," it can not be determined from which tissue or cells that the library of previously obtained spectra are to be obtained prior to steps (a)-(d) and from what source the tissue and cells are to be derived. As claim 12 has been cancelled, the rejection as to this claim is now moot. In reference to claim 1, upon reviewing the specification, one skilled in the art would be aware that the library of previously obtained spectra would include those cells and/or tissues that are the subject of the particular analysis and are obtained from individuals that may exhibit the particular cellular abnormality. For example, if a diagnosis is to be made of skin cancer, analyses/spectra of such skin cancer cells/tissues obtained from individuals with skin cancer could serve as the particular reference.

It is also asserted in the Action that claims 1, 5 and 7-12 are vague and indefinite due to recitation of "correlating the reflected light spectrum with a disease state." It is asserted that it can not be ascertained how correlating the reflected light spectrum with a disease state leads to a diagnosis of a disease state in a living organism. Applicants respond that the pending claims are sufficiently definite to the skilled artisan with respect to the recitation of "correlating the reflected light spectrum with a disease state," as evidenced, for example, by the data presented in Exhibit A and discussed herein.

Further, as explained in the specification, the stain taken up by diseased cells, such as those found in dysplasia, pre-cancer and cancer, stained according to the methods described therein will exhibit a metachromatic shift, the extent of which can be determined from spectrophotometrically-obtained data. As clearly explained in the specification at, for example, page 22, lines 1-5, and in amended claim 1, one can compare the extent of the metachromatic shift in the test sample spectra with that obtained from the library of previously obtained spectra of similarly stained tissue or cells. The samples upon which the library is based have been previously diagnosed by conventional techniques as described in the specification and thus a correlation as to disease state of the test sample may be easily made by such comparison of metachromatic shift of the test sample and that from the reference sample. Withdrawal

of the rejection of claims 1, 5 and 7-12 under 35 U.S.C. § 112, second paragraph, is respectfully requested.

Rejection of claims 1-19 under 35 U.S.C. § 102(b)

Claims 1-19 stand rejected under 35 U.S.C. § 102(b) over U.S. Patent No. 5,784,162A (Cabib et al.), as evidenced by Vaezy et al. [*Journal of Microscopy* 163:85-94 (1991)] and Marchesini et al. [*Photochemistry and Photobiology* 55:515-522 (1992)]. Cabib et al. is relied on in the Action for teaching spectral imaging methods for *in situ* medical diagnosis and treatment comprising preparing a sample to be imaged, viewing the sample through an optical device optically connected to a spectrometer, collecting and measuring incident light using a detector and collecting and interpreting data using a mathematical algorithm.

As only claims 1, 5 and 7-11 remain pending after entry of this amendment, the rejection as to claims 2-4, 6 and 12-19 is now moot. Withdrawal of the rejection of these non-pending claims under 35 U.S.C. § 102(b) is respectfully requested. As to the remaining, pending claims 1, 5, and 7-11, applicants assert that the rejection under 35 U.S.C. § 102(b) is improper. As the issue date of U.S. Patent No. 5,784,162A to Cabib et al. (July 21, 1998) is less than a year prior to the filing date of the present application (May 5, 1999), Cabib et al. is not prior art under 35 U.S.C. § 102(b) and applicants respectfully request withdrawal of the rejection of claims 1, 5 and 7-11 over 35 U.S.C. § 102(b) over Cabib et al.

Accepting, *arguendo*, the Action's characterization of the teachings of Cabib et al., there is absolutely no teaching or suggestion in Cabib et al. of a method of diagnosing a disease state *in situ* in biological tissue or cells of a living organism that includes, for example, comparing the degree of the metachromatic shift of the dye from the reflected light spectrum of the stained tissue or cells with the degree of the metachromatic shift of the dye from a library of previously obtained spectra of similarly stained tissue or cells as recited in amended claim 1. As no such limitation is taught or suggested in Cabib et al., and as Vaezy and Marchesini fail to supply any of the deficiencies of Cabib et al., applicants respectfully assert that claims 1, 5 and 7-11 are

patentable over Cabib et al., and that no rejection under any section of 102, Title 35, or any other section of Title 35, is proper.

In light of the foregoing discussion, it is believed that claims 1, 5 and 7-11 are in condition for immediate allowance. Action towards this end is respectfully requested. The Examiner is invited to telephone the undersigned attorney regarding any issues that may be handled in that fashion.

Respectfully submitted,

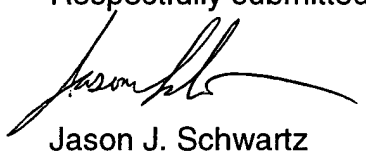

Jason J. Schwartz
Registration No. 43,910

HALE AND DORR LLP
1455 Pennsylvania Avenue, N.W.
Washington, DC 20004-1008
(202) 942-8490
Date: March 5, 2002

APPENDIX 1

IN THE SPECIFICATION:

Please amend the paragraph on page 4, lines 20-25, as follows:

--Toluidine blue O will rapidly and intensely stain [metaplasic] metaplastic, [precancerous] pre-cancerous, and cancerous lesions when applied topically and these lesions are readily seen by the deep blue color. Normal healthy tissue is stained very little, if at all. This slight excess stain is easily removed where stained lesions remain (stained) for a period of time. The staining of cancerous and [precancerous] pre-cancerous lesions on application of toluidine blue O occurs within a minute.--

Please amend the paragraph on page 4, line 27 to page 5, line 2, as follows:

--There are three mechanisms (not mutually exclusive) of staining that have been suggested by the research to date: 1) [mucopolysaccaride] mucopolysaccharide staining with metachromasia (a concomitant shift in the absorption spectra of the phenothiazine compound)[,]; 2) enhanced nuclei and nucleoli staining (RNA- and DNA-rich) associated with enhanced proliferation of these organelles in pre-cancerous and cancerous cells; and[,] 3) enhanced staining of the mitochondria of [metaplasic] metaplastic ([dysplasic] dysplastic, pre-cancerous, and cancerous) cells.--

Please amend the paragraph on page 5, lines 19-24, as follows:

--Despite the apparent sensitivity of methylene blue for [metaplasic] metaplastic cells and tissue, toluidine blue O, also a thiazine dye, has found more widespread application. Sugerman, et al. (*Arch. Surg.* 1970 Mar.;100(3):240-3[]) uses toluidine blue in the diagnostic stain of neoplastic lesions. Chesser, et al. (*J. Dermatol. Surg. Oncol.* 1992 Mar.;18(3):175-6) recommend using toluidine blue O, *ex vivo*, as a staining technique for the treatment of adenoid cystic carcinoma by Mohs micrographic surgery.--

Please amend the paragraph on page 8, lines 14-20, as follows:

--The histochemical pathology of [dysplasic] dysplastic, pre-cancerous, and cancerous lesions that would be expected to be stained with any of the thiazine dyes[,] will vary as to the degree of *metachromasia* within the cell tissue layer. This depends on the variation in mucin production, aberration of nuclei, nucleoli, and mitochondrial organelle distribution, as well as changes in cell membrane permeability, charge structure and membrane transport properties, etc., with the various cell[s] types associated with each diagnosis and the stage of metaplasia or cell transformation.—

Please amend the paragraph on page10, lines 17-22, as follows:

--U.S. Patent [5,748,162] 5,784,162 teaches [of] multi-variant spectral bio-imaging analysis for diagnostics and therapy utilizing optical means including two-dimensional photodetector arrays. Requiring sample preparation and visualization, the method incorporates, in part, fluorescent dyes to enhance imaging but makes no reference to the utility of spectrum analysis of metachromasia or differential biological staining of tissue or cells as a means of correlating [metaplasic] metaplastic stage.--

Please amend the paragraph on page 10, lines 24-29, as follows:

--U.S. Patent 4,973,848 uses a pair of laser beams in the course of photodynamic therapy where one beam is used to analyze the surface to be treated as a means of controlling the properties of the "treatment' beam but makes no reference to the utility of spectrum analysis of metachromasia or differential biological staining of tissue or cells as a means of correlating [metaplasic] metaplastic stage. Further, the analysis is limited to the wavelength of the analysis laser beam rather than a broad spectrum of light energy.--

Please amend the paragraph on page 11, from lines 1-6, as follows:

--Complex biological stain compositions for histological examinations are taught in U.S. [patent] Patent No. 4,595,582. These dyestuff compositions, of which some components are of the thiazine family, are an improvement to conventional histochemical methods, enhancing visualization of cytological structure within fixed tissue. It does not teach or make reference to the utility of spectrum analysis of metachromasia or differential biological staining of tissue or cells as a means of correlating [metaplasic] metaplastic stage.--

Please amend the paragraph on page 20, lines 1-17, as follows:

--The use of biological stain in direct staining *in vivo* has been shown to have a high degree of sensitivity to a variety of [metaplasic] metaplastic, pre-cancerous and cancerous cells and tissues. For example, the thiazine dyes toluidine blue O and methylene blue have found frequent use in the *in vivo* diagnosis of oral epithelial carcinomas, dermal epithelial carcinomas, esophageal cancer, cervical and vaginal cancers, and even in the detection of bladder cancers. However, the specificity of the staining process in differentiating between the stage and type of metaplasia has been variable and has not allowed for a definitive diagnosis of the [Disease State] disease state. Generally, vital or [in vivo] *in vivo* staining has not been able to distinguish between normal cellular repair process and metaplasia. Practitioners have used the sensitivity of the stains to locate diseased tissue and then subsequently relied on biopsy and classical histochemical techniques for a final diagnosis. Histochemical methods further rely on staining the morphological as well as the biochemical features retained after the fixation and sectioning of the tissue sample. The staining features of intensity and color are then examined and a subjective, if skilled, determination as to the underlying cell type is rendered as the diagnosis.--

Please amend the paragraph on page 21, line 29 to page 22, line 20, as follows:

--The analysis of the reflectance spectrum of the stained tissue area by software means is significant to the present invention. It may be conducted in a variety of ways to fulfill the intent of this method. For example, the software analysis of the spectra may compare the metachromatic shift of the stain toluidine blue O between two or more specific wavelengths by correlation. The results are then compared to a body of data previously collected and correlated to underlying conventional histochemical data defining the cellular stage of metaplasia. It can readily be seen that a combination of two stains, for example, methylene blue and pyronin Y, applied either from one composition or applied as two separate preparations and analyzed by comparative spectrometric means and suitable software analysis, may afford a desirable degree of enhanced specificity in certain applications. The two stains would compete for certain histochemical features that would distinguish cells undergoing normal repair processes and those cells that are [metaplasic or neoplasic] metaplastic or neoplastic. Further additional diagnostic utility may be afforded by means of monitoring the [photo oxidation] photooxidation of the specific stain or stain composition by spectrometric means and analyzing the resulting change in the spectra, correlating the result to underlying clinical analysis of the procedure verified by conventional means. The [photo oxidation] photooxidation may be by means of a broad-spectrum high intensity light source (either through the fiber optic bundle or external to the fiber optics), a filtered high intensity light source, or by means of a specific wavelength laser. In this manner of analysis, the change in the characteristic spectrum of the measured tissue stain combination (in other words, the [photo bleaching] photobleaching process; i.e., *"photochromasia"*[.]) may be followed as a function of time, intensity, or a combination thereof.

Please amend the paragraph on page 22, line 27 to page 23, line 10, as follows:

--It can be further seen that this *in situ* diagnostic method may be extended to a highly controlled [photo therapeutic] phototherapeutic method for the destruction and removal of diseased tissue and cells. It has been seen that many biological stains, for example, particularly the thiazine family, such as methylene blue and toluidine blue O, [has] have found application as photosensitizers for photodynamic therapy. Because of the specificity of these biological stains for [metaplasic] metaplastic cells, including cancerous cells, the [photo oxidation] photooxidation results in a cytotoxic effect. It may be highly advantageous to the practitioner to be able to assess the cytological state of an area of tissue in applying irradiation for [photo therapeutic] phototherapeutic means, for example, allowing discrimination between highly [metaplasic] metaplastic tissue as compared to inflamed but otherwise normal tissue area and cells undergoing the normal repair processes. This would minimize, for example, the amount of tissue destruction by means of a high power laser. Further, the course of the phototherapy up to a defined end point can be accurately and carefully assessed using the combination of biological stain/photosensitizer and a spectrometer means of analyzing the stain *in situ*.--

IN THE CLAIMS:

Please cancel claims 12, 13 and 17-19 and please amend claims 1, 5 and 7-11 as follows:

1. (Thrice Amended) A method for diagnosing [a disease state] dysplasia, pre-cancer or cancer [in situ] *in situ* in biological tissue or cells of a living organism, comprising:

a) applying to the tissue or cells *in situ* a [thiazine] dye selected from the group consisting of methylene blue and toluidine blue O;

b) removing excess dye from the tissue or cells;

c) generating a reflected light spectrum from the tissue or cells by illuminating the stained tissue or cells with light;

d) directing the reflected light spectrum to a spectrometer;

e) comparing the degree of the metachromatic shift of the dye from the reflected light spectrum of the stained tissue or cells with the degree of the metachromatic shift of the dye from a library of previously obtained spectra of similarly stained tissue or cells; and

f) correlating the reflected light spectrum with a disease state, whereby an [in situ] *in situ* diagnosis of [a disease state] dysplasia, pre-cancer or cancer is made.

5. (Twice Amended) A method as in [Claim] claim 1, wherein said comparing comprises the use of a digital microprocessor.

7. (Twice Amended) A method as in [Claim] claim 1, wherein the tissues or cells are thought to be [diseased or metaplastic].

8. (Amended) A method as in [Claim] claim 1, wherein the spectrometer is able to measure light for a range of or some part of a range of wavelength from 200 to 1100 nanometers.

9. (Twice Amended) A method as in [Claim] claim 1, wherein the reflected light spectrum is measured and recorded, and said measuring comprises the use of a photometer and one or more light filters.

10. (Twice Amended) A method as in [Claim] claim 1, wherein the tissues or cells are [of[from at least one organ selected from the group consisting of [the] skin, cervix, vagina, mouth, colon, esophagus [or] and internal organs.

11. (Twice Amended) A method as in [Claim] claim 1, wherein, prior to said comparing step, a reflected light spectrum from unstained tissue or cells is subtracted from the spectrum of the stained tissue or cells.

APPENDIX 2

1. (Thrice Amended) A method for diagnosing dysplasia, pre-cancer or cancer *in situ* in biological tissues or cells of a living organism, comprising:

a) applying to the tissue or cells *in situ* a dye selected from the group consisting of methylene blue and toluidine blue O;

C8 b) removing excess dye from the tissue or cells;

c) generating a reflected light spectrum from the tissue or cells by illuminating the stained tissue or cells with light;

d) directing the reflected light spectrum to a spectrometer;

e) comparing the degree of the metachromatic shift of the dye from the reflected light spectrum of the stained tissue or cells with the degree of the metachromatic shift of the dye from a library of previously obtained spectra of similarly stained tissue or cells; and

f) correlating the reflected light spectrum with a disease state, whereby an *in situ* diagnosis of dysplasia, pre-cancer or cancer is made.

C9 5. (Twice Amended) A method as in claim 1, wherein said comparing comprises the use of a digital microprocessor.

Amd D1 7. (Twice Amended) A method as in claim 1, wherein the tissues or cells are thought to be metaplastic.

C10 8. (Amended) A method as in claim 1, wherein the spectrometer is able to measure light for a range of or some part of a range of wavelength from 200 to 1100 nanometers.

9. (Twice Amended) A method as in claim 1, wherein the reflected light spectrum is measured and recorded, and said measuring comprises the use of a photometer and one or more light filters.

10. (Twice Amended) A method as in claim 1, wherein the tissues or cells are from at least one organ selected from the group consisting of skin, cervix, vagina, mouth, colon, esophagus and internal organs.

C 10

11. (Twice Amended) A method as in claim 1, wherein, prior to said comparing step, a reflected light spectrum from unstained tissue or cells is subtracted from the spectrum of the stained tissue or cells.

Hyperspectral analysis of methylene blue or toluidine blue O staining of freshly excised human tissue

Materials and Methods

Tissue Samples

Patients scheduled for Mohs surgery were enrolled for the use of discard (tumor de-bulking) tissue for metachromatic stain imaging.

Instrumentation

The multispectral image system utilized incorporates a 1.3 megapixel 12 bit monochrome CCD imager (Q Imaging Corporation) co-axial to a monochromatic light source (Schott linear variable interference filter). This is directed though a cubic beam splitter with orthogonal linear polarization. A 55 mm Telecentric lens is used in combination with a 2x teleconverter for a primary magnification of 0.75 X. The field of view (FOV) 11.5 mm x 9.2 mm to an array of 1280 by 1024 pixels, with each pixel mapping approximately 9 microns of image to 7 microns of image sensor.

Wavelength selection was controlled by a linear translation stage stepper motor driven under computer control in conjunction with image acquisition. A 1 Ghz Pentinum III processor was used with 512 MB ram to acquire and process the image cube using proprietary software developed with Visual Basic 6.0. The LVF monochromator provides 27 – 10 nm stepped bands with an average spectral half power band width of 14 – 18 nm. Under the low illumination conditions of this optical arrangement, acquisition of all 27 frames in the image cube requires approximately 90 seconds.

Staining procedure

Freshly excised bulk discard tissue was pre-rinsed in 1% acetic acid for 30 to 60 seconds using forceps and 60 mm Petri dishes. Maintaining orientation of the cut margin, the tissue was then immersed in either 0.1% or 0.05% Methylene Blue (USP) for 30 to 60 seconds and rinsed again in 1% acetic acid for 30 to 60 seconds. Toluidine blue O was used at a concentration of 0.1% The tissue section was placed on a standard microscope slide with the cut margin facing down. A second slide or cover slip was placed on top of the sample to "hold" the tissue flat to the lower slide.

The sample was then placed on the stage of the multispectral camera and adjusted for the best field of view. The 27 band multispectral image set was then acquired under software control and the tissue sample was then processed by conventional histological techniques (cryostat, fixation and automated staining with either toluidine blue O or Haematoxylin-Eosin) for later examination and comparison of pathology to the spectral image set.

Preliminary spectral image analysis

During this feasibility study, a number of parameters were varied in order to ascertain and evaluate both proper operation of the instrument/software system as well as to determine a preliminary staining protocol. The following image sets are from a sequence of samples where the parametrics remained relatively constant.

Images sets from samples 01.024, 01.025, and 01.027 are presented and discussed below.

Results

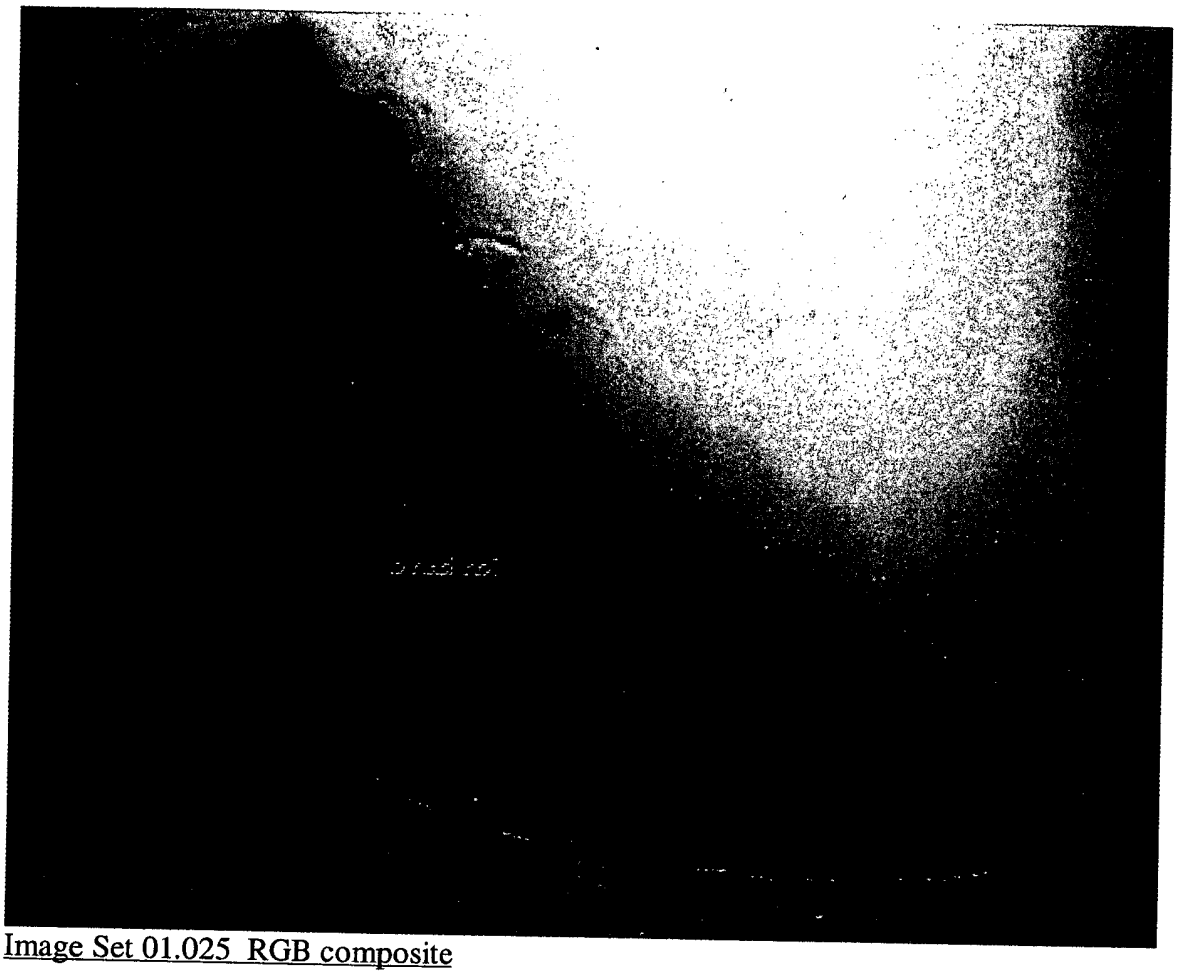

Image Set 01.025 RGB composite

Sample 01.025 was taken from a pre surgical biopsy diagnosed BCC excision as de-bulked (discard) tissue, immediately pre-rinsed and stained for 60 seconds in 0.05% methylene blue (MB) and post-rinsed. Post surgical histopathology of fixed sections from this specimen were examined and found to be normal tissue with some apparent inflammation. No specific BCC (basal cell carcinoma) pathology was observed.

This sample serves as a reference to the properties of MB staining of freshly excised human tissue. Full 27 band spectra were collected and analyzed graphically. Three regions of interest (ROI) are selected here and plotted in the ROI graph 01.025 on the following page. The label colors ("named" accordingly) correspond to the spectral selection graph plots.

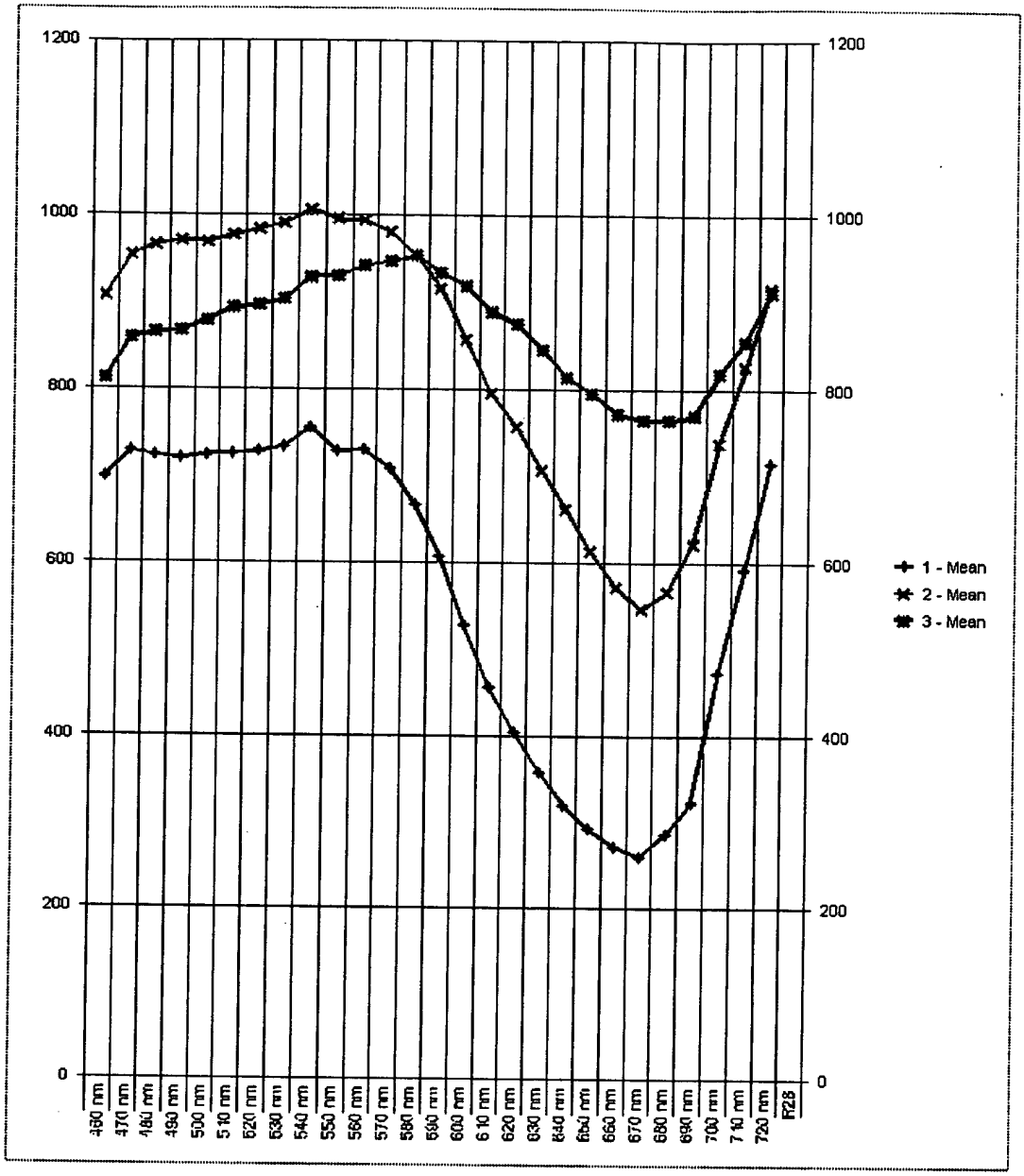

ROI Graph 01.025

The most intense apparent staining is graphed as the "red ROI". Peak absorption♦ at 670 nm corresponds closely to the peak absorption of aqueous MB at 665 nm. Green and blue ROI's are of correspondingly lower staining intensity. Note the 630 nm feature in the red ROI spectra. The very slight metachromasia suggested here is assigned to "inflammation".

♦ As presented graphically, "increasing" absorption of light by the stain "decreases" the recorded light intensity. The Y axis in the graphs represents raw pixel response to light; the lower values corresponding to lower reflected light detected and "greater" absorption. Hence the "peak" absorption is a trough in these graphs.

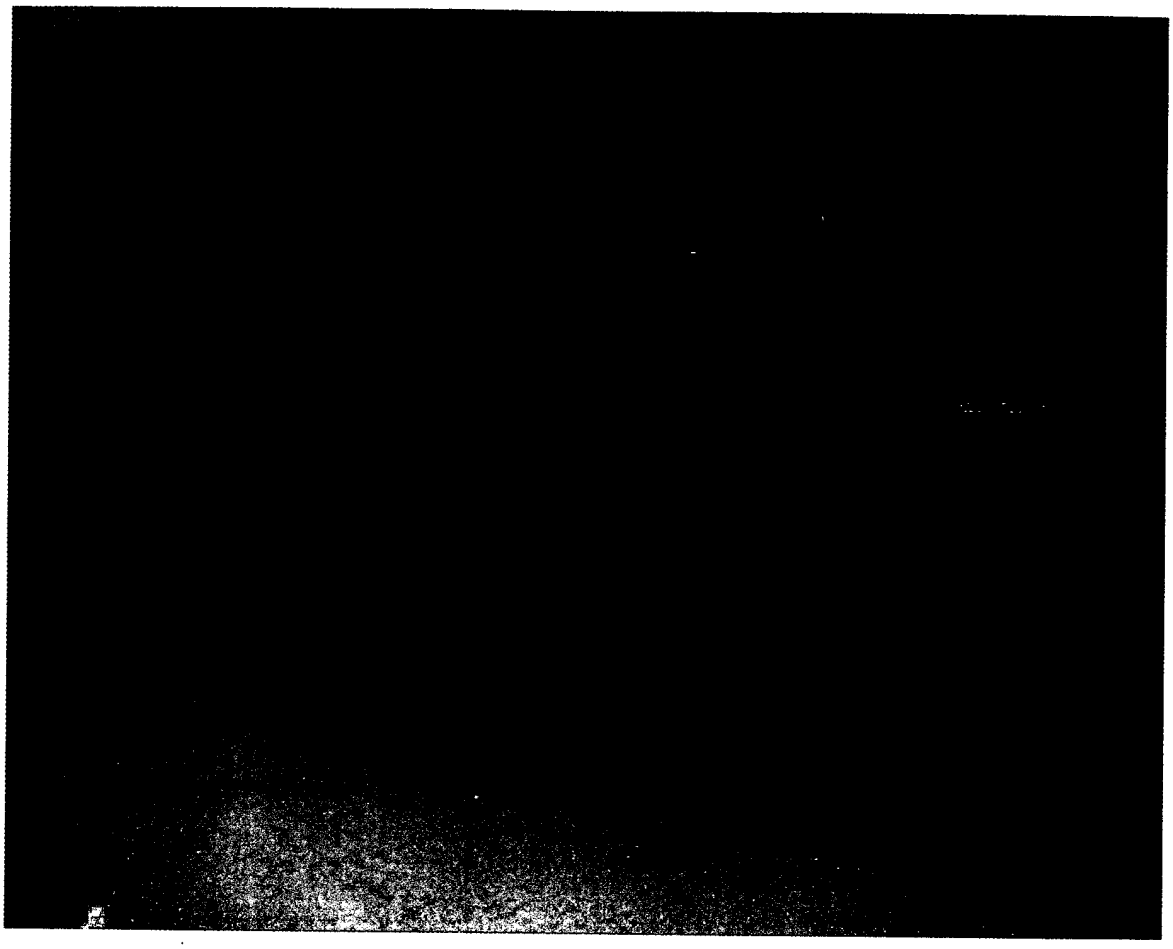

Image Set 01.024.2.2 RGB composite: ROI set 1

Sample 01.024 was a large section of tissue imaged in a total of 6 sets. Set 2.2 is shown here as typical of the entire specimen. Histopathology reveals the "entire section" to be basal cell carcinoma. Because this sample is almost entirely tumor, it serves as a good direct comparison to sample 01.025 as a normal tissue sample. Three "regions of interest" are arbitrarily selected and the corresponding spectral responses are plotted in the following graph (page 7).

The "red ROI" is probably most typical of an extensive cluster of BCC tumor cells. Note that the spectral regions at 640 nm and 610 nm are of greater relative absorption than the 670 nm band that typically corresponds to methylene blue monomers. Dimerization of MB increases the absorption around 610 nm; increasing polymer aggregates of thiazine stains are known to shift the absorption peak further toward the blue end of the spectrum. These results might suggest that cancer cells preferentially concentrate MB due to the intercellular chemistry and enhanced cell membrane permeability. Dye interaction with the more highly electronegative cell membranes of cancerous and pre cancerous tissue may also shift the absorption spectrum toward the blue.

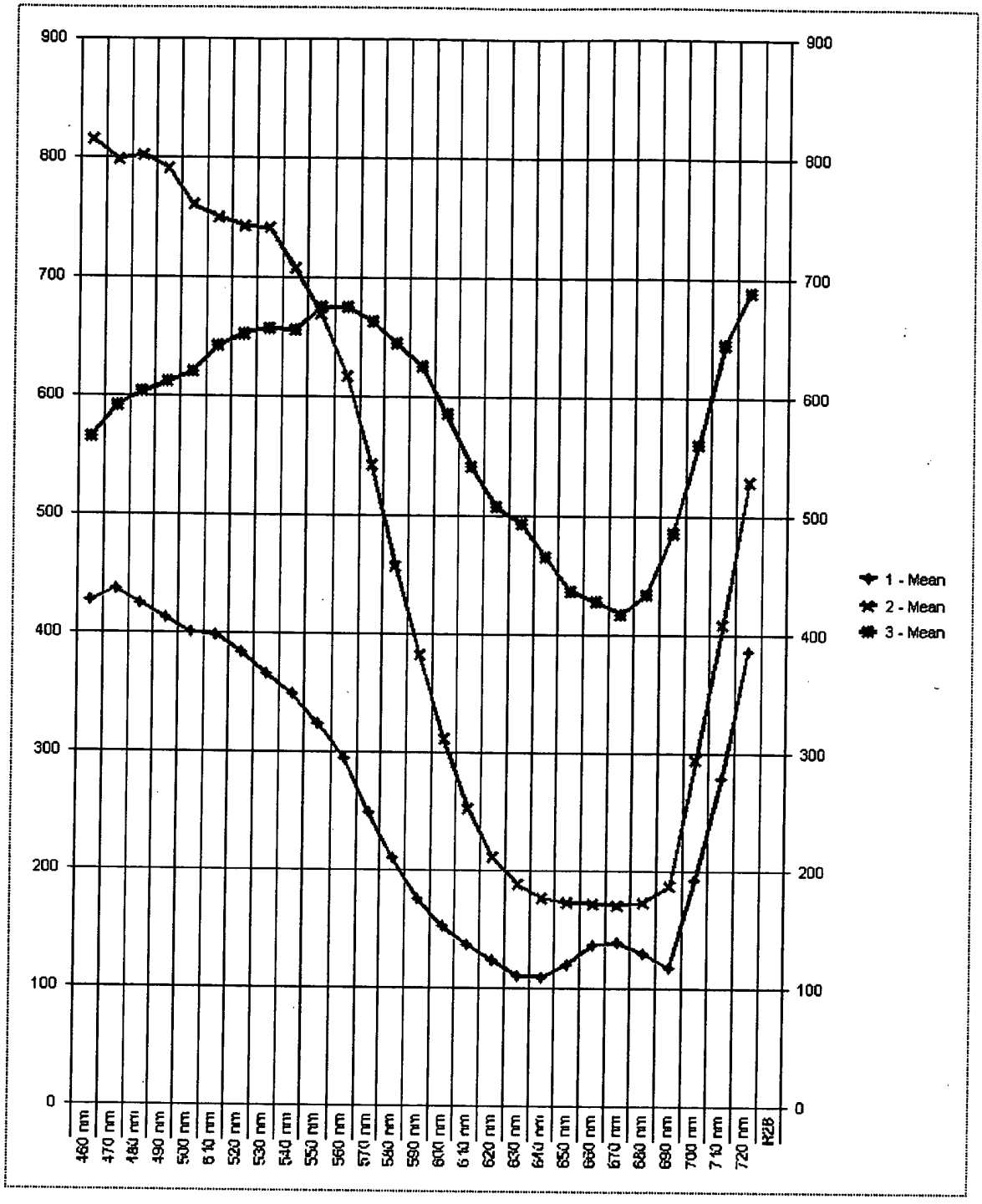

ROI Graph 01.024.2.2 : set 1

Three selected ROI's as discussed above.

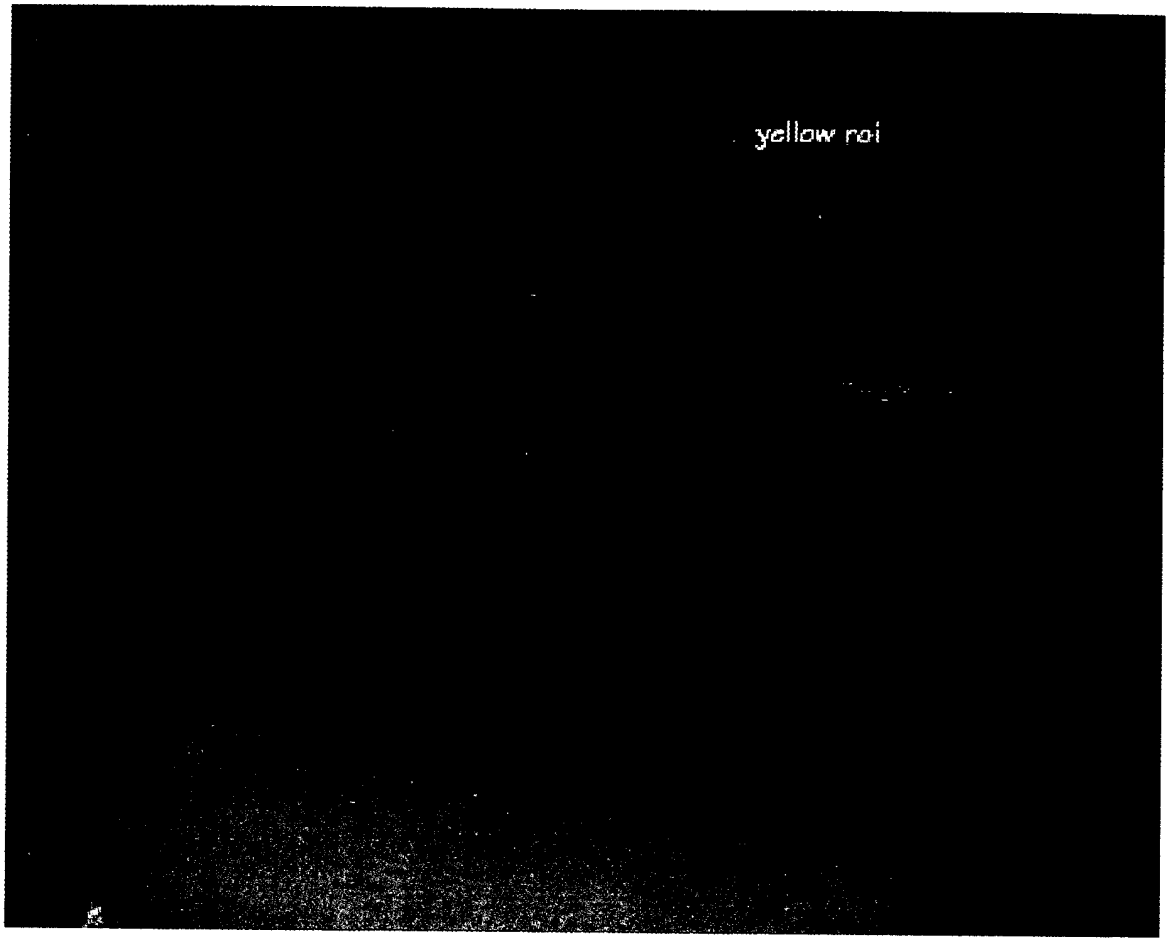

Image Set 01.024.2.2 RGB composite: ROI set 2

Because this section is clearly BCC, another interesting feature can be examined. This tissue sample was not immediately processed and was allowed to remain in air for approximately 15 minutes. Consequently the residual blood clotted in the tissue and could not be completely removed by pre-rinsing prior to staining. The coagulated hemoglobin can be seen in this image set and was selected for spectral response analysis, plotted in the following graph (page 9) together with other ROI's similar to the previous selections. The characteristic hemoglobin spectra can be recognized, despite not being corrected from raw pixel count data. Graphical analysis of potential interference with MB spectra can be made to some extent. This issue is addressed in greater detail further in this report.

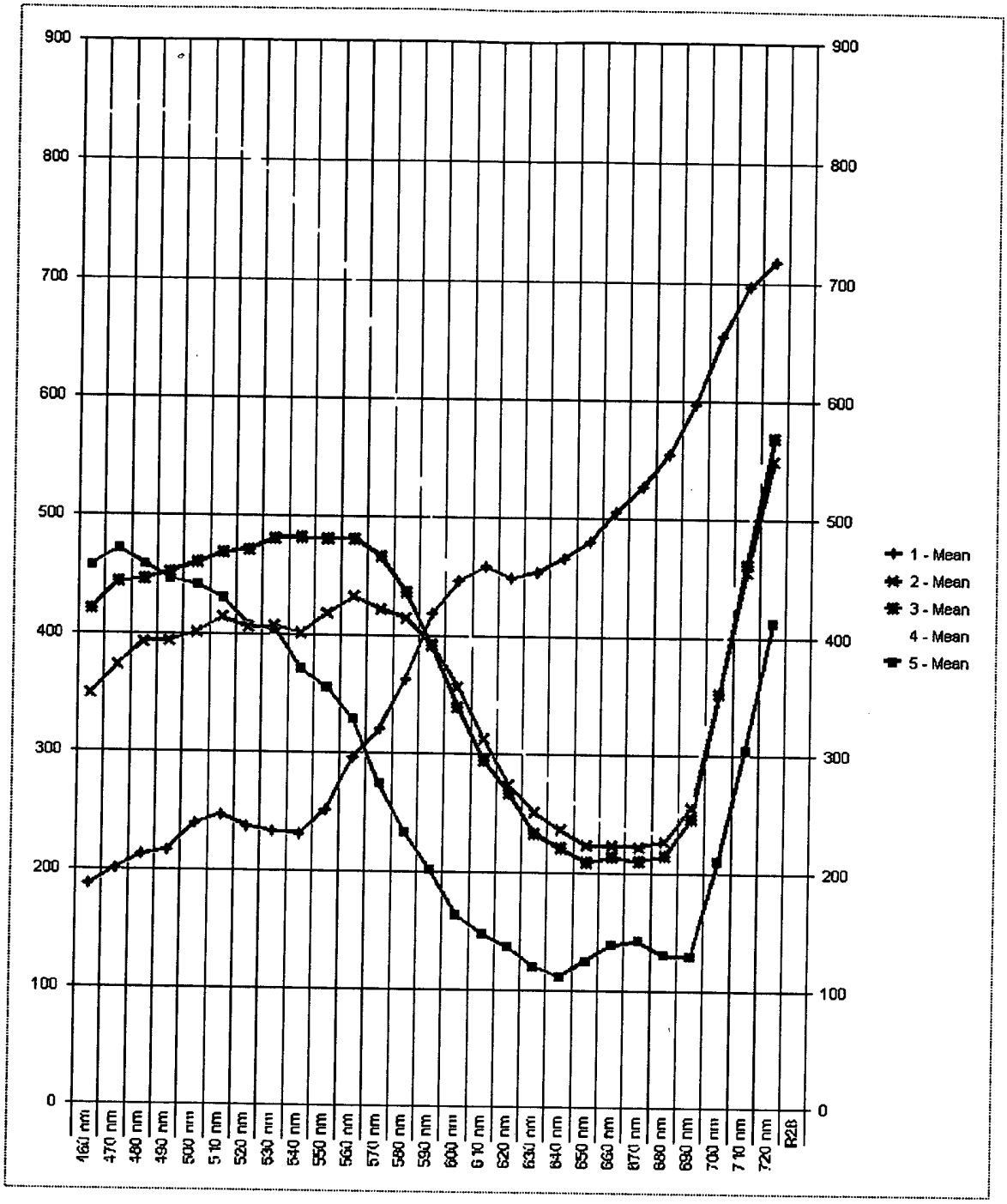

ROI Graph 01.024.2.2 : set 2

A hemoglobin spectrum is seen in the red ROI plot; little evidence of MB spectra is apparent here. Successive ROI's on shifted MB regions are seen to have a lower absorption in the 460 nm to 560 nm region where heme would have the great absorption. Any interference of heme with the principal metachromatic shift bands would, in this comparison, appear limited.

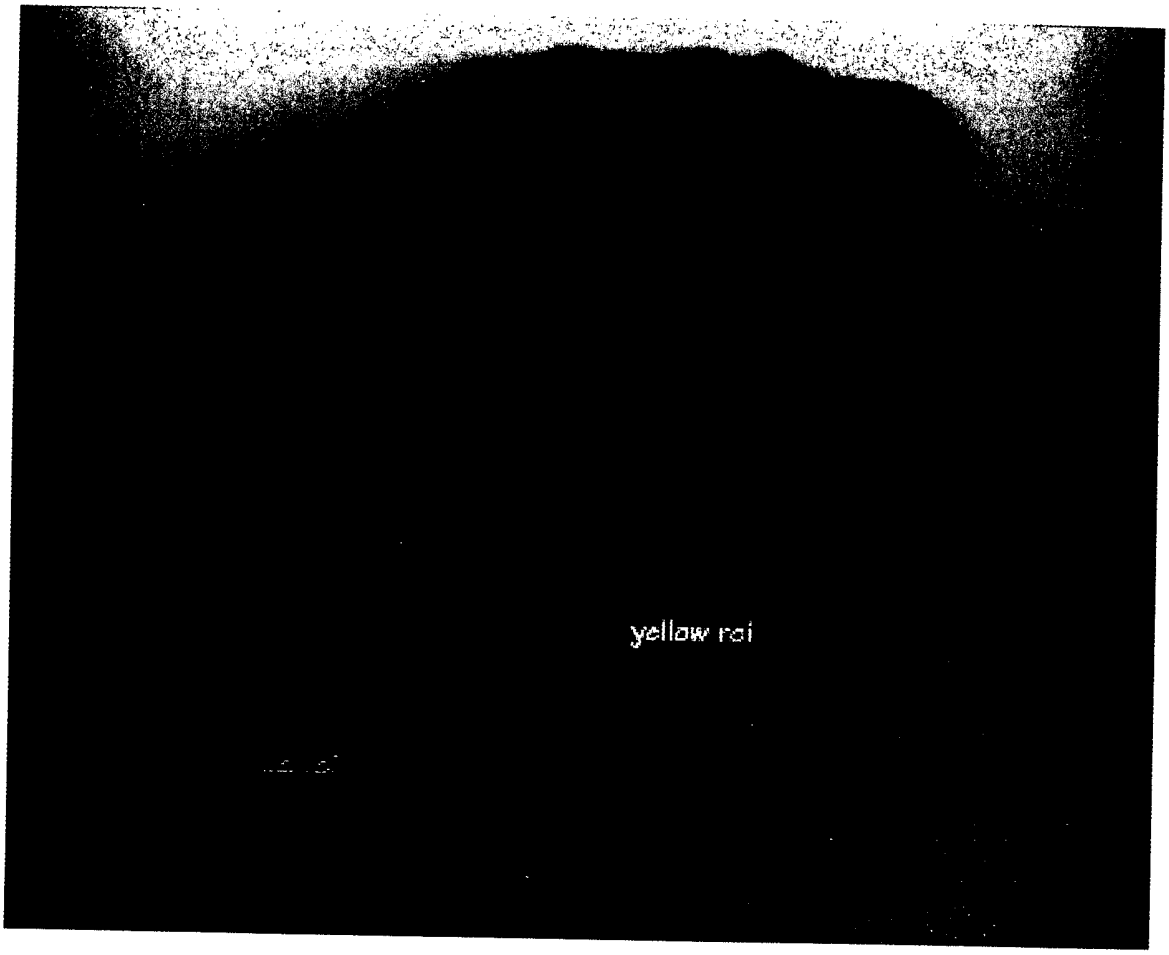

Image Set 01.027 RGB Composite

Histopathology of sample 01.027 reveals "small regions of basal cell carcinoma with associated inflammation". Four regions with significant absorption at 670 nm were selected and the corresponding spectra are plotted below (page 11). The "red ROI" clearly displays significant metachromatic shift toward the shorter wavelengths comparable to the spectra of the BCC spectra in sample 01.024.2.2. Less significant metachromasia is apparent in the green and blue ROI spectra. The spectra of the yellow ROI would appear more typical of the inflammation seen in sample 01.025, having less absorption in the range 610 nm to 640 nm.

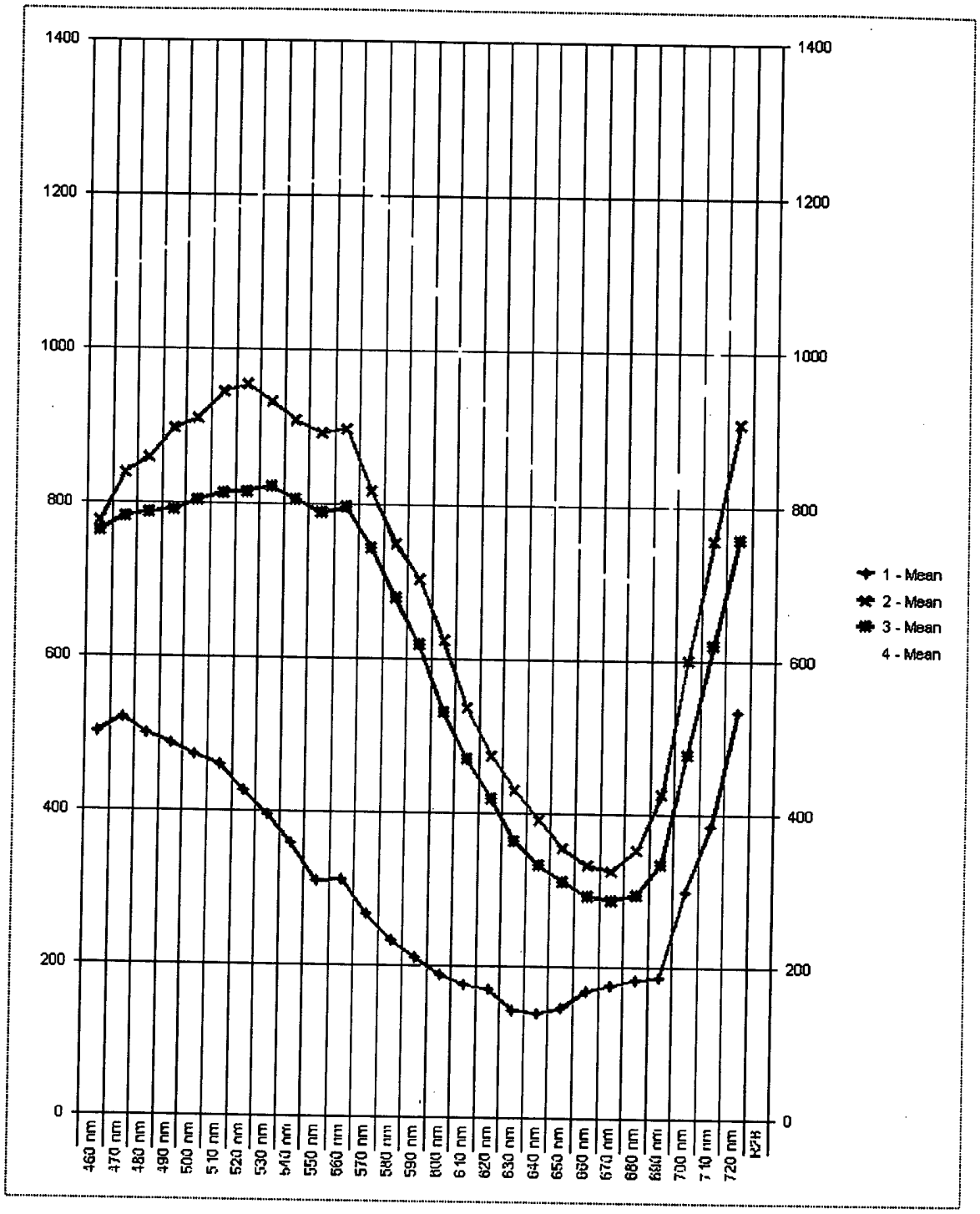

ROI Graph 01.027

See discussion above.

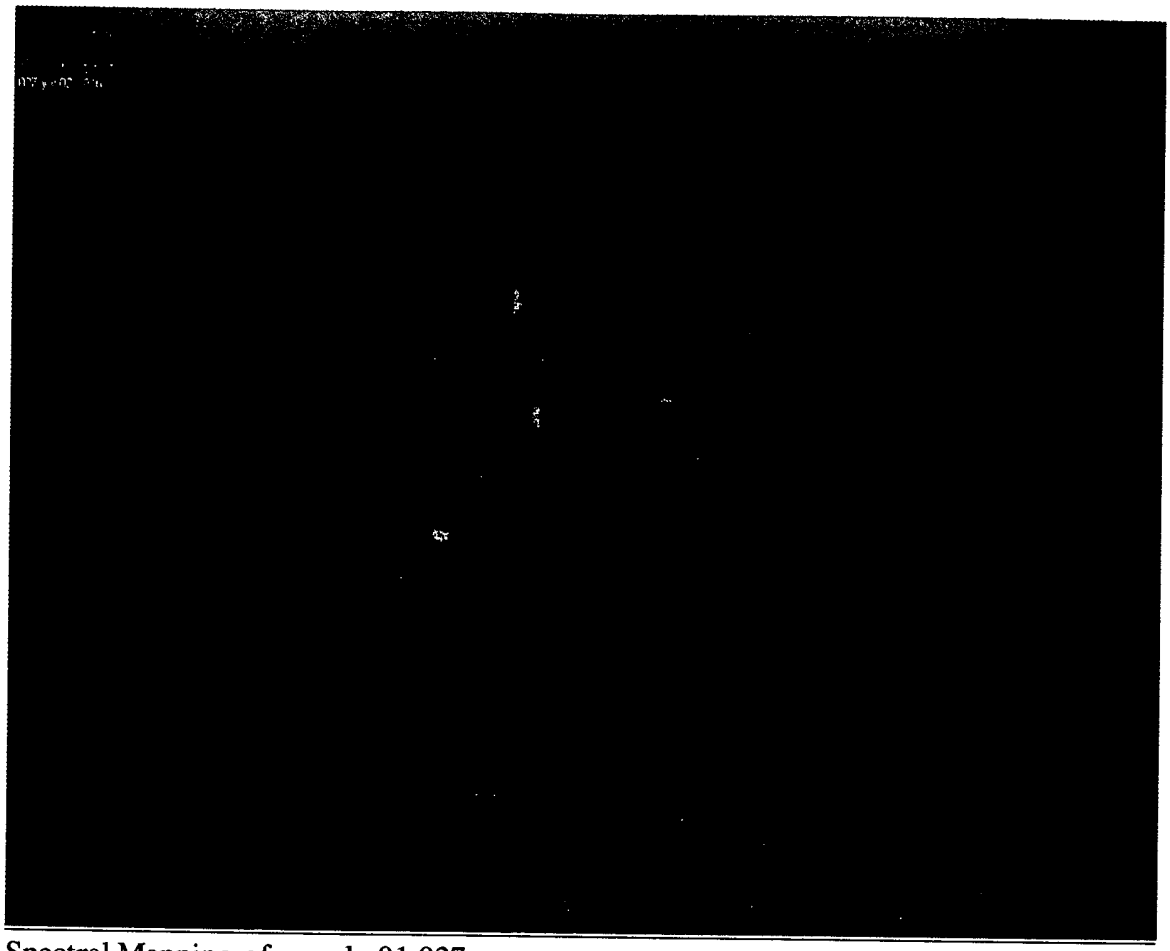

Spectral Mapping of sample 01.027

The spectra from sample 01.027 were evaluated using a series of 3 band subsets and processed by a feature selection algorithm, where the spectral features are propagated back through the entire image and then "painted" (false color mapping) on a pixel by pixel basis. In this mapping, four subsets based on the relative intensity of the 610, 640 and 670 nm bands were defined and mapped. Note that these selected colors do not correspond to the spectra plotted in the previous graphs. The red ROI is a "range" selected feature and actually excludes areas displaying "significantly higher" metachromatic properties. However, on close inspection (not readily seen in this image reproduction) the red features are found in isolated clusters on both the lower right edge as well as the central areas – also mapped with feature selection analysis. Those areas mapped in yellow and green are of spectral features displaying less apparent metachromasia than the red ROI; whereas the blue mapped areas are those bordering between inflammation (little metachromasia) and features comparable to known BCC staining.

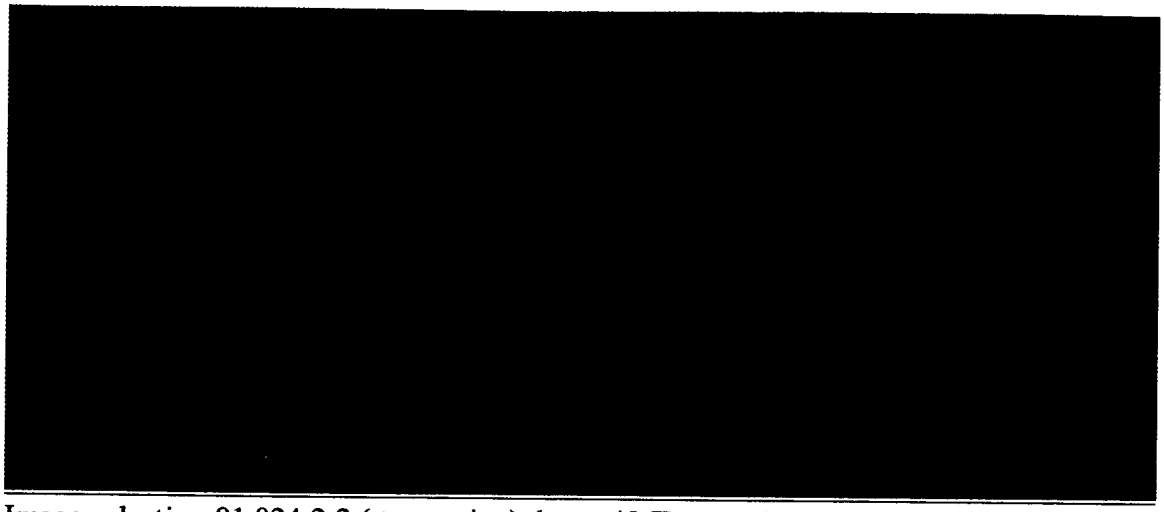

Image selection 01.024 2.2 (top region): heme / MB metachromasia

A series of spectral plots were made across the image cube in those regions marked on this RGB composite of image sample 01.024.2.2. Close inspection shows a sequence going from left to right starting over an area that appears to be primarily heme. The purpose of this spectral sequence is to qualitatively evaluate the potential inference of the heme spectra with that of the metachromatic properties of MB staining of apparent BCC lesions.

There are seven ROI's selected, from left to right, and plotted in the following graphs (page 14) directly from the image software system.

The red plot corresponds to the left most ROI and appears to be primarily heme with little evidence of MB absorption. Moving right, the next ROI is plotted as green, followed by blue, yellow, magenta, light blue and the right most ROI plotted below as the black graph.

The spectral features observed in the range from 460 nm to 560 nm progressively decrease in absorption, suggesting a decrease in associated heme spectra. The influence of any absorption on the range from 630 nm to 690 nm, the principal regions of MB and associated metachromasia, appears minimal. Note the peak absorption in this series for MB (at roughly 635 nm) remains approximately the same. It would suggest smearing of the blood across the tissue sample in this area that is associated with BCC lesions.

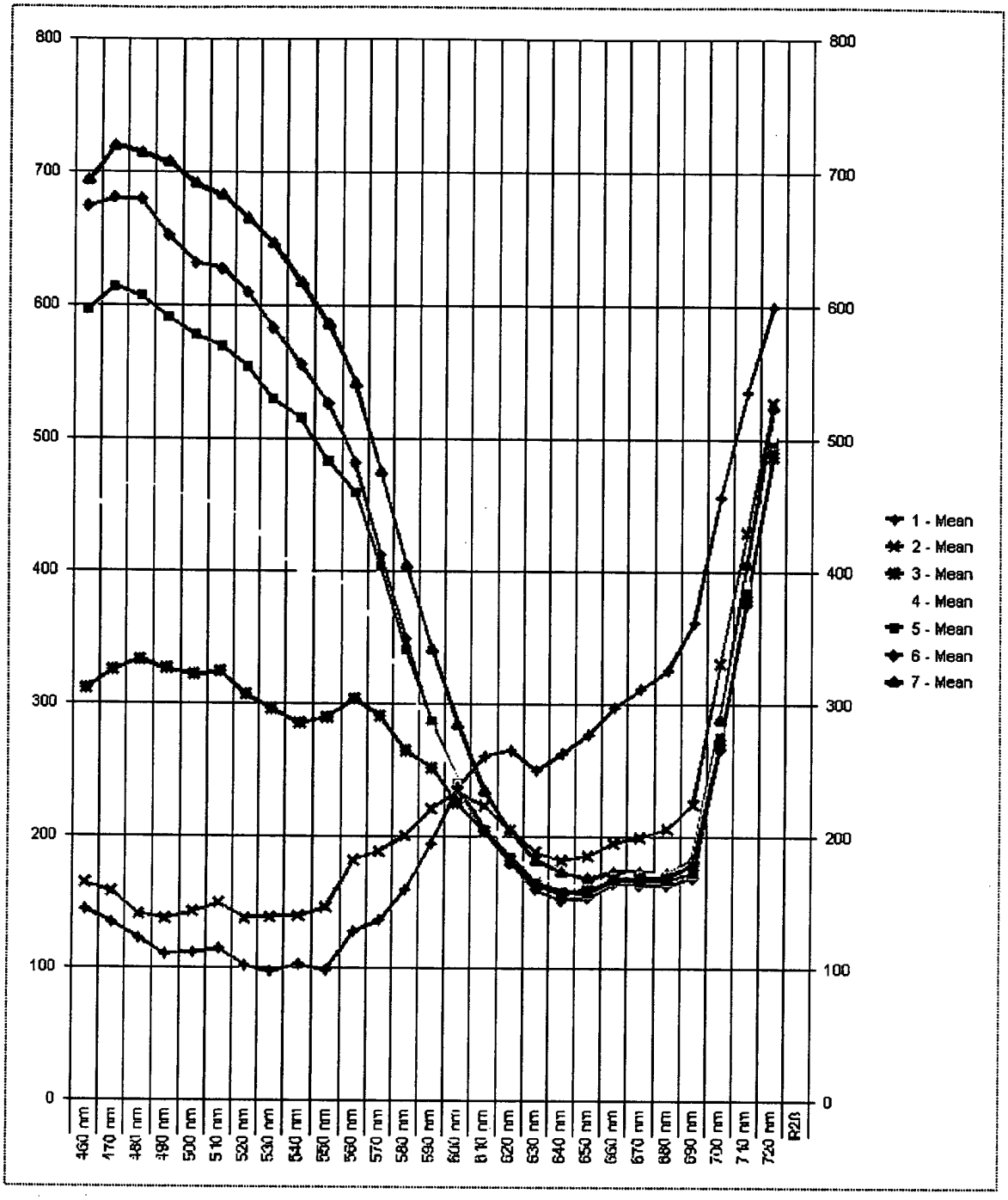

ROI Graph: sub image 01.024.2.2

See discussion on previous page.

Metaspectral analysis of methylene blue staining of freshly excised surgical tissue

From the preliminary evaluation of the multispectral image sets, an empirical determination of key spectral features consistent through the sample sets was made. For those samples displaying a positive metachromatic spectral signature and which correlate with subsequent histopathological diagnosis, the following key features were noted:

The principal absorption spectrum (for methylene blue) centers near 665 to 670 nm and displays a metachromatic shift with an increase in absorption toward the yellow/green wavelengths. By inspection, principal noted features are "shoulders" centered near 600 nm and 640 nm which often exceed the peak absorption intensity at 670 nm. These features correspond to known spectral shifts of MB either resulting from charge-charge association of the dye molecule with electronegative membranes and/or resulting from dimer and oligomer formation of the dye itself. The metachromatic shift resulting from some "active" dye uptake differentiates from normal tissue which characteristically excludes the cationic thiazine dyes (clinical literature). These spectral features are herein defined as metachromatic indices (MI) and the corresponding analysis as "**metaspectral**[♦]" as follows:

MI Class 1: where the relative intensity at 610nm is equal to or exceeds that at 640 nm and 670 nm respectively.
MI Class 2: where the relative intensity at 640 nm is equal to or exceeds that at 670 nm; 610 nm being less than that at either 640 or 670 nm
MI 01 (600≥610): a sharp shoulder where the relative intensity at 600 nm is equal to or exceeds 610 nm; both bands having less relative intensity than 670 nm.
MI 45 (640≥650): a sharp shoulder where the relative intensity at 640 nm is equal to or exceeds that at 650 nm; both bands having less intensity than 670 nm.
Negative MI (MIØ): no indication of peak broadening to wavelengths shorter than the center wavelength of 670 nm.

MI 01, MI 45, and MI Class 2 are ***2 band*** analysis referenced to the 670 nm band. MI Class 1 is a ***3 band*** analysis. MI 01 is an implicit subset of MI Class 1 and MI 45 is an implicit subset of MI Class 2. These defined indices form a continuum of metachromasia based spectral signatures that have been correlated with histopathology by empirical means.

A subset of samples from 01.001 through 01.027 were used for the creating this "library" of spectral signatures or metachromatic indices. (The principal samples used were 01.019, 024, 025, and 027; these samples being well correlated to the histopathology.) They were then tested against the balance of the first set of samples to determine how well the correlation is made. Subsequent samples, from 01.028 on, were then evaluated using this set of MI's and scored against the results of conventional histology.

♦ Metaspectral is defined as distinct from hyperspectral; hyperspectral analysis being based on a spectral band subset determined within the data set based on parameters within the given dataset, whereas the spectral band subset for metaspectral analysis is determined by the features of the stain-tissue interaction.

Of a total of 41 tissue sets obtained in the UCHSC study (some with multiple samples from a given incision), 29 complete sets of data were obtained (and 5 sets for toluidine blue O). Remaining samples were omitted from this comparison because the spectral image data was missing or corresponding histopathology was not obtained (thin sections were not obtained). The data is presented in tabular form in Table 1 (UCHSC MB MI analysis) on the following page (page 17).

Table 1. University of Colorado Health Sciences Center methylene blue metachromatic index analysis.

Sample#	type	Stain	pretrt/ stain /destain sec-sec-sec	location	Delay to stain (min)	Pathology		MI class 1	MI class 2	MI 01	MI 45	MI 0
01.003	bcc	0.05% MB	30-30-30	nose	5	Nd			+	+	+	
		0.1% MB			10	Nd		+		+	+	
01.004	bcc	0.1% MB	30-30-30	nose	3	Small tumor sections	+			+	+	
01.005	bcc	0.1 % MB	30-30-30	forehead	2	Possible tumor, uncertain	+/-			+	+	
01.006	bcc	0.1% MB	30-30-30	shin	2	Tangential epidermis, uncertain	+/-			+	+	
01.011	scc inv	0.05% MB	30-30-30	hand	55	Nd					+	
01.013	Bcc	0.05% MB /s	30-30-30	ear	16	Retraction centered tumor	+			+		
01.014	Bcc	0.05% MB /s	30-30-30	nose	3	All tumor	+			+	+	
01.015	scc inv	0.05% MB /s	30-30-30	scalp	15	Inflammation, uncertain tu	+/-	+		+	+	
01.017	bcc	0.05% MB	30-30-30	scalp	2	Negative (All normal)	-					
01.018	bcc	0.05% MB	30-30-30	ear	2	Half tumor	+			+	+	
01.019	bcc	0.1% MB	30-30-30	cheek	15	All tumor	+			+	+	
01.020	bcc	0.1% MB	30-30-30	lip	11	Lower half tumor	+				+	
01.021	bcc	0.1% MB	30-30-30	cheek	27	All tumor	+			+	+	
01.022	bcc	0.1% MB	30-30-30	helix	6	1.1 all tumor	+			+	+	
"		0.1% MB				1.2 all tumor	+				+	
01.024	bcc	0.05% MB	60-45-60	left nasal alar	5	1.1 Mostly tumor;	+		+		+	
"						1.2 mostly tumor	+		+		+	
01.025	bcc	0.05% MB	60-60-60	left nose	10	Negative (Normal)	-					
01.026	scc in situ	"	60-60-60	left forehead	1	Bowen's scc in situ	+		+		+	
01.027	bcc	"	60-60-60	left eye	2	Sections of tumor, edge & central	+		+		+	
01.032	bcc	"	60-60-60	rt orbital rim	7	Negative	-					
01.033	bcc	"	60-60-60	pre auricular	2	Negative/ Small BCC*	+		+		+	
01.034	bcc	"	60-60-60	nose	2	Patches of BCC	+	+	+			
01.036	bcc	"	60-60-60	finger	2	Positive on edge	+		+		+	
01.037	bcc	"	60-60-60	nose	45	Distributed BCC buds	+		+	+	+	
01.038	bcc	"	60-60-60	cheek	35	Negative (thick section)	-					
01.039	bcc	"	60-60-60	alar	25	Multiple BCC sections	+	+	+	+	+	
01.040	bcc	"	60-60-60	shin	3	Negative	-					

Bcc: basal cell carcinoma; **Scc**: squamous cell carcinoma; **Nd**: no data (either pathology and/or image data); **/s** with saline solution; **inv**: invasive

Discussion

Table 1 summarizes the data from twenty six samples and a total of twenty nine separate multispectral image data sets, all using MB and evaluated using a defined set of spectral features (metachromatic indices). All samples were "debulked" tissue sections obtained from a Mohs surgical procedure; the surgical site was determined by prior biopsy and it can be anticipated that most, if not all of the excision samples are positive for either basal or squamous cell carcinoma. Of the 26 samples, 5 samples were found by standard histopathology to be negative.

Using the set of defined metachromatic indices for MB, all samples were evaluated by applying the MI to the multispectral data sets. Significant regions of interest (ROI's) are mapped to the image sets by selection; positive matching of the MI is indicated in Table 1 (one or more of the last five columns).

Initially one false positive was observed with sample 01.033. Microscopic histochemical examination was scored "negative". The image set scored a moderate MI 45 and MI Class 2 ROI (see following plates). The corresponding thin section was re-evaluated microscopically; on careful re-examination a small loci of cells typical of basal cell carcinoma was observed at the approximate loci indicated by the image mapping algorithm.

With this set of MI's applied to all 29 image sets, no false negative was observed.

MI Class metaspectral image mapping: representative samples of the MI image mapping algorithms defined are given in the following plates (pages 19 and 20). Each photonegative image in the left column is mapped in dark blue corresponding to those voxels matching MI 45 (where the relative intensity at 640 nm equals or exceeds that at 650 nm). The corresponding image in the right column is mapped in light blue together with the MI 45 map and either a MI 01 (where the relative intensity at 600 nm equals or exceeds that at 610 nm) or with MI Class 2 (where the relative intensity at 640 nm equals or exceeds that at 670 nm).

01.021 MI 45 map
basal cell carcinoma from cheek

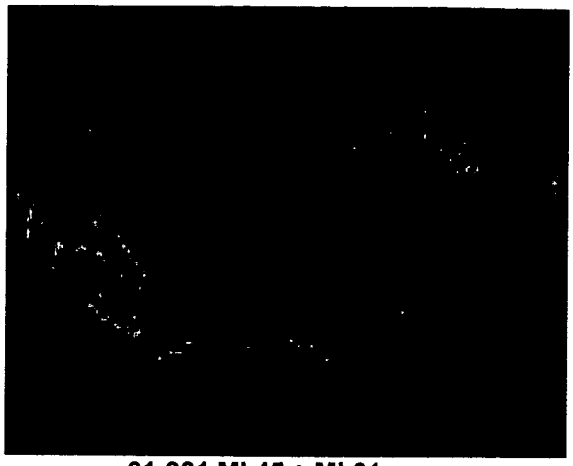

01.021 MI 45 + MI 01 map

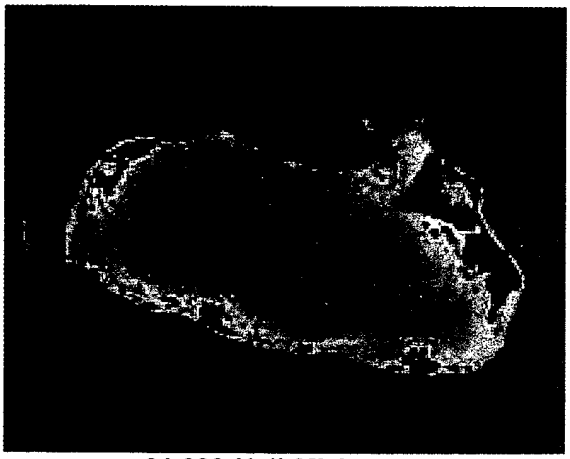

01.022 (1.1) MI 45 map
basal cell carcinoma, helix

01.022 (1.1) MI 45 + MI Class 2 map

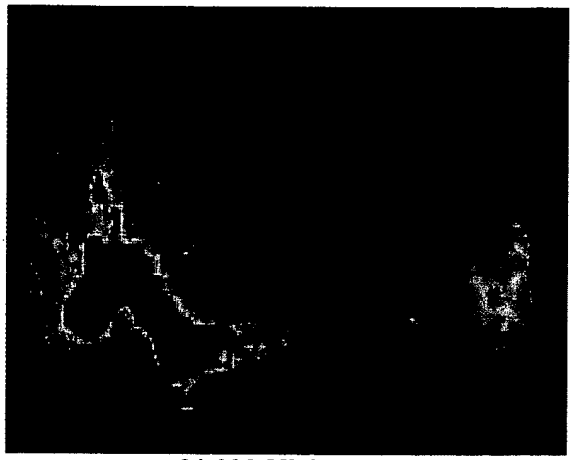

01.033 MI 45 map
basal cell, pre auricular

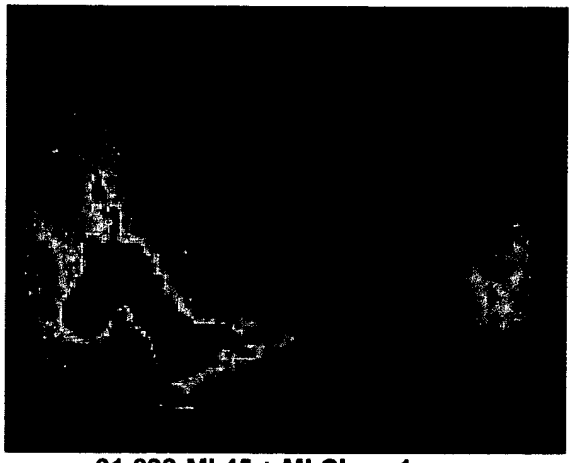

01.033 MI 45 + MI Class 1 map

01.036 MI 45 map
basal cell, finger

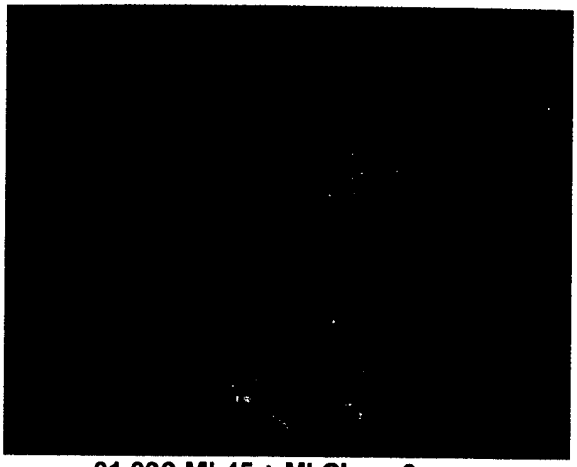

01.036 MI 45 + MI Class 2 map

01.037 MI 45 map
basal cell, nose

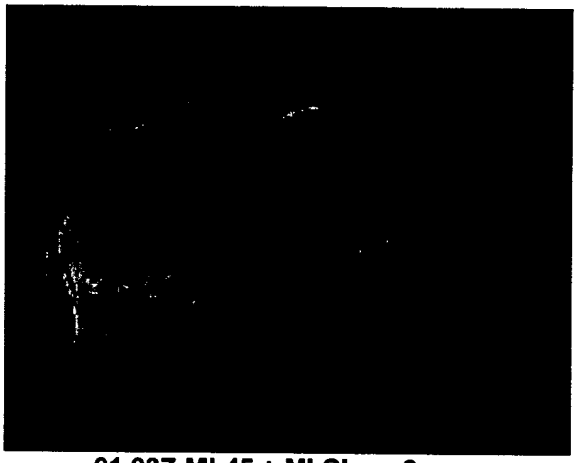

01.037 MI 45 + MI Class 2 map

Metaspectral analysis of toluidine blue O staining of freshly excised surgical tissue

A similar analysis was performed on a subset of clinical samples (5 samples) using toluidine blue O as the metachromatic stain. The principal absorption spectrum of toluidine blue O (TBO) centers near 635 to 640 nm and displays a metachromatic shift as an increase in absorption toward the yellow/ green wavelengths. By inspection, the principal noted feature is centered near 600 nm (see red graph below). In the samples stained with TBO in this present study, the shoulder at 605 nm never exceeded the relative intensity of the main peak at 640 nm. In most areas with relatively limited dye uptake, no distinct shoulder was observed. The metachromatic shift (in this instance the shoulder at 605 nm) resulting from "active" dye uptake differentiates cancerous from normal tissue which characteristically excludes the cationic thiazine dyes (clinical literature).

For reference, an RGB color composite of sample 01.008 is presented together with corresponding region of interest (ROI) multispectral plots corresponding to various areas with differing TBO stain intensity.

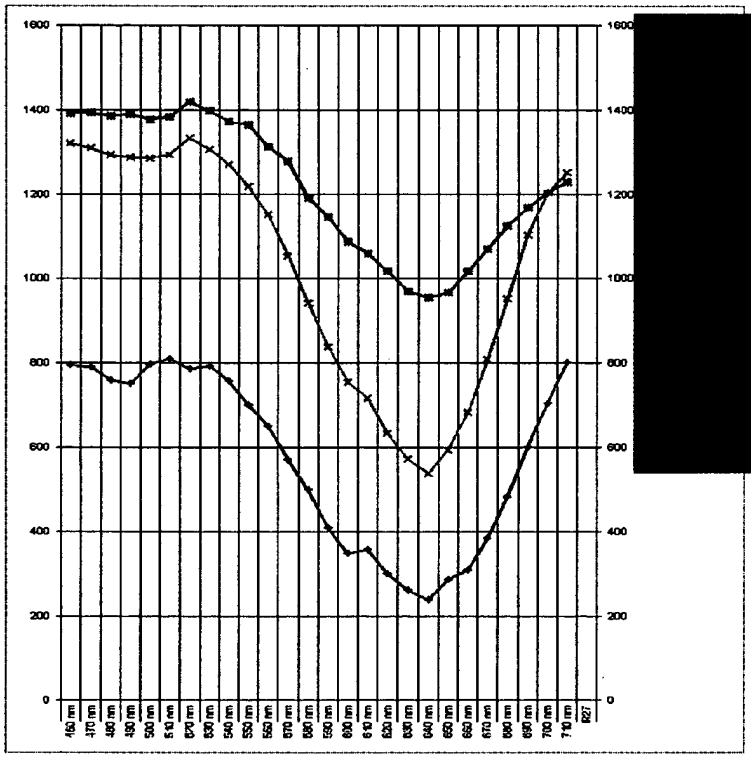

The red multispectral plot is sampled from the most intense blue stained regions (just right of the center of the tissue sample) seen in the accompanying RGB image on the right; the green is sampled from the perimeter of the region; and the blue is sampled from the more diffuse, lightly blue stained area in the upper left portion of the tissue. Using this feature to define an MI for TBO, the remaining samples were evaluated using the MI 01 feature. The results are presented in Table 2 on the following page (page 22).

Table 2. University of Colorado Health Sciences Center toluidine blue O metachromatic index analysis.

Sample#	type	Stain	pretrt/ stain /destain sec-sec-sec	location	Delay to stain (min)	Pathology		MI class 1	MI class 2	MI 01	MI 45	MI 0
01.007	bcc	0.1% TBO	30-30-30	cheek	5	**1.1 All tumor in center (circular sebaceous gland)**	+			+		
"						**1.2**	+			+		
01.008	bcc	0.1% TBO	30-30-30	scalp	3	**Uncertain small section marked**	+			+		
01.009	scc invasive	0.1% TBO	30-30-30	temple/ear	20	**retraction, certain tumor;**	+			+		
01.010	bcc	0.1% TBO	30-30-30	forehead	25	Nd				+		
01.023	bcc	0.1% TBO/a&e	30-30-30	nose	5	Nd						

Bcc: basal cell carcinoma; **Scc**: squamous cell carcinoma; **Nd**: no data (either pathology and/or image data); **a&e**: 1% acetic acid & 5% ethanol

MI Class metaspectral image mapping: representative samples of the MI image mapping algorithms defined for Toluidine blue O (TBO) are shown for two of the samples. Each photonegative image in the left column is mapped in dark blue corresponding to those voxels matching MI 01 (for TBO, equivalent to that derived for methylene blue) (where the relative intensity at 600 nm equals or exceeds that at 610 nm). The corresponding image in the right column is mapped in light blue together with the MI 01>640 map where the 600/610nm absorption intensity is greater than that at 640 nm.

01.008 TBO M01 map
basal cell, scalp

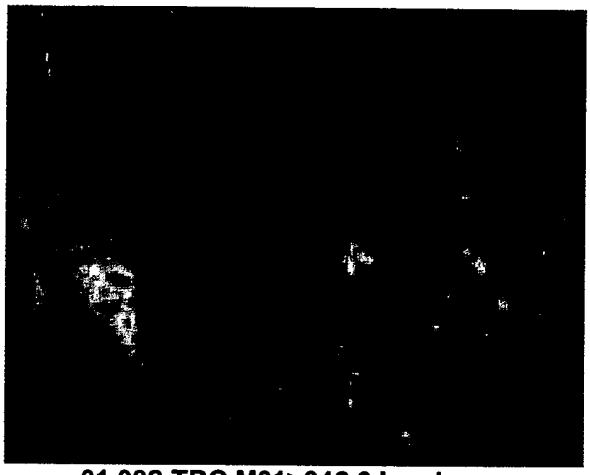

01.008 TBO M01>640 3 band map

01.009 TBO M01 map
scc invasive, temple/ear

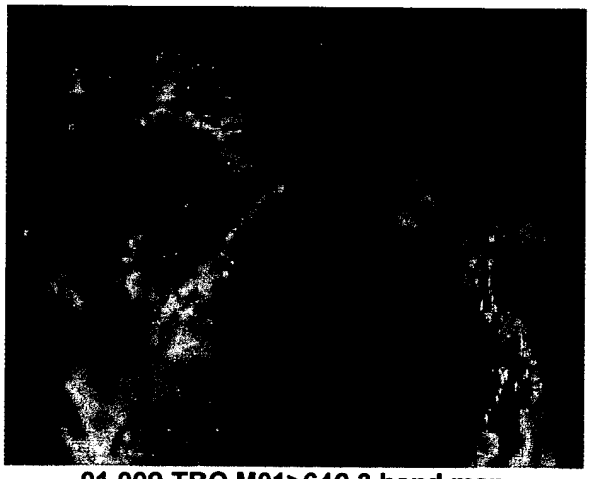

01.009 TBO M01>640 3 band map

Clinical review

Localization of islet cell tumors of the pancreas: A review of current techniques

Ihor J. Fedorak, MD, Tien C. Ko, MD, Donald Gordon, MD, Michael Flisak, MD, *and* **Richard A. Prinz, MD,*** *Maywood, Ill.*

Operative exploration with attempted curative resection should be attempted on virtually all patients with islet cell tumors of the pancreas who do not have metastatic disease evident on preoperative studies. Because of the small size and variable location of many of these neoplasms, localization studies play an important role in ensuring appropriate and successful surgical therapy. A review of currently available preoperative and intraoperative aids for tumor localization is presented. A new technique of selective intraarterial injection of methylene blue is described along with a report of our preliminary results. Further evaluation and use of this technique and other newly developed technologies are warranted to lower the commonly reported 10% to 30% negative exploration rate for these sometimes elusive tumors. (SURGERY 1993;113:242-9.)

From the Department of Surgery, Medicine and Radiology, Stritch School of Medicine, Loyola University, Maywood, Ill.

CURATIVE RESECTION IS THE OPTIMAL therapy for islet cell tumors of the pancreas. Within the past three decades this therapeutic goal has become attainable for most patients with no evidence of metastatic disease. Several large series have documented cure rates of 90% or more with resection of insulinomas.[1,2] Complete tumor removal can be accomplished in 30% to 40% of patients with gastrinomas, with one series documenting an immediate biochemical cure rate as high as 82%.[3,4] Although experiences with other functioning islet cell tumor types are limited, curative resections have been reported for vipomas[2] and somatostatinomas.[5] Although resection for cure is often not possible in most patients with glucagonomas, tumor debulking can decrease circulating glucagon levels and palliate symptoms.[6]

Careful operative exploration remains the most sensitive method of localizing pancreatic islet cell tumors. Patients with a certain biochemical diagnosis of a functioning tumor who are reasonable operative candidates should undergo operation by an experienced surgeon even though results of preoperative localizing studies are equivocal or noncontributory. Nevertheless, the small size and variable location of these neoplasms pose special challenges to the surgeon. The availability of accurate and sensitive preoperative and intraoperative localization studies has played a major role in recent improvements in surgical cure rates. Currently ultrasonography,[1,7] computed tomography,[2,8] angiography,[9-11] magnetic resonance imaging,[12] and percutaneous selective portal venous sampling,[13-20] are advocated by different groups as sensitive and useful means of identifying the site of these tumors before operation.

Despite use of these techniques, failure to resect tumor because of the inability to localize it before operation or at laparotomy still occurs in 30% to 35% of patients with gastrinomas[21,22] and 7% to 10% of patients with insulinomas.[3,23] Better localization techniques may help detect these obviously small and potentially curable neoplasms. Herein we review results attainable with currently available noninvasive and invasive localization procedures and discuss newly developing techniques, including a method we have recently begun to investigate, selective intraarterial methylene blue injection based on selective arterial stimulation testing.

Accepted for publication March 18, 1992.

Reprint requests: Richard A. Prinz, MD, Loyola University Medical Center, 2160 S. First Ave., Maywood, IL 60153.

0039-6060/93/$1.00 + .10 11/55/40834

NONINVASIVE TESTS

Ultrasonography. Ultrasonography is an attractive option for localization of islet cell tumors because of its simplicity, noninvasiveness, and relatively low cost. However, the technique is greatly operator dependent, as evidenced by the wide variation in results. In a recent report from the Mayo Clinic, 13 of 18 (72%) patients with islet cell carcinomas studied with ultrasonography underwent successful localization of their tumors.[8] No mention was made of the size of the tumors, but islet cell carcinomas are typically much larger than most insulinomas and many gastrinomas. The same authors reported a 59% sensitivity for preoperative localization with ultrasonography in 36 patients with insulinomas. They suggested that only preoperative ultrasonography is needed before an initial abdominal exploration for an insulinoma if intraoperative ultrasonography is available. Insulinomas were successfully resected from 100% of their patients managed in this fashion.[1] Gunther et al.[7] reported similar results with preoperative ultrasonography and recommended it as the initial step in localization.

Other investigators have reported much less success with ultrasonography. Fraker and Norton[3] at the National Institutes of Health (NIH) found that only seven of 32 (22%) patients had islet cell tumors successfully localized by preoperative ultrasonography.[3] Sensitivities of 25% or less have been documented by Vinik et al.[20] in a series of 40 patients with insulinomas treated at the University of Michigan and by Wise et al.[24] in a series of 23 patients with gastrinomas treated at Ohio State University. Both of these groups conclude that the low yield of ultrasonography makes routine screening for islet cell tumors with this technique unwarranted. Our own experience is similar to these latter investigators. Therefore we no longer rely on preoperative ultrasonography to localize islet cell tumors.

Computed tomography. Computed tomographic scanning is the most widely used noninvasive technique for initial localization of islet cell tumors. Dynamic scanning during contrast infusion with 4 to 5 mm cuts is the procedure of choice to detect a mass or possible tumor blush.[12] In addition to being more sensitive than plain computed tomographic scanning, dynamic scanning gives more three-dimensional information, such as the relationship of the tumor to the pancreatic or common bile ducts.[25]

Localization results with computed tomography have varied between series. The highest sensitivity has been reported by Thompson et al.[8] from the Mayo Clinic, where 23 of 24 (96%) patients with islet cell carcinomas had their tumors localized on preoperative computed tomography. This accuracy is unusually high and may be attributable to the relatively advanced stage of disease of the patients in this series. Although no tumor sizes were reported, only 11% of the patients were amenable to curative resection. In a series from the Cleveland Clinic, Broughan et al.[2] reported accurate localization of islet cell tumors by computed tomography in 10 of 18 (56%) patients examined. Stark et al.[12] were able to localize seven of 11 (64%) tumors in their series using computed tomography.

Several large series have suggested that computed tomography is more sensitive in localizing gastrinomas compared with insulinomas. Fraker and Norton[3] found that computed tomography accurately localized 22 of 37 (59%) gastrinomas and 6 of 14 (43%) insulinomas. Comparable results for insulinoma localization by computed tomography have been reported in a more recent series from the Mayo Clinic, where eight of 23 (35%) patients examined had tumors accurately localized by computed tomography.[1] Vinik et al.[20] reported less favorable results, with only four of 27 (15%) patients having accurate preoperative localization of their insulinomas by computed tomography.[20] Broughan et al.[2] and Dunnick et al.[26] have had better success, reporting more than 60% sensitivities for the ability of computed tomography to localize insulinomas.

The sensitivity of computed tomography to accurately localize islet cell tumors is dependent on the size and location of the neoplasm. Unfortunately, few series report tumor size and location, making comparisons difficult. This is especially true when evaluating techniques for localizing gastrinomas. Wise et al.[24] reported a sensitivity of 29% for computed tomography in localizing gastrinomas. In this series 11 of the 22 gastrinomas located were extrapancreatic, with a mean size of 1.3 cm in the localized group and 0.6 cm in the nonlocalized group. Howard et al.[27] could only localize three of 10 gastrinomas by computed tomography. Multiple tumors that were not identified were present in two of these three. However, Deveney et al.[21] accurately localized gastrinomas in 13 of 16 (81%) patients, with all nonvisualized tumors being less than 1 cm in size. Thus computed tomography can be expected to accurately identify roughly one third to two thirds of primary gastrinomas, with results highly dependent on the location and size of the tumor. Computed tomography does have the additional advantage of a very high sensitivity for identifying liver metastases from gastrinomas, which

aids in tumor staging. Several series have reported that 70% to 100% of liver metastases can be identified with computed tomography.[12, 21, 28]

Computed tomography has also been the primary means by which nonfunctioning islet cell tumors are localized.[29] These tumors are usually large, with sizes of 3 to 24 cm in the largest series.[30] In our series of nonfunctioning islet cell carcinomas, six of the eight patients had palpable tumors on physical examination.[29] The large size allows a 96% to 100% sensitivity for localization by computed tomography.[29, 30]

Magnetic resonance imaging. Magnetic resonance imaging has become widely available in recent years and has been used for localization of islet cell tumors. Preliminary results of its effectiveness are now becoming available. Wise et al.[24] found a 20% sensitivity and 100% specificity for magnetic resonance imaging, which are similar to this group's results with computed tomography. Frucht et al.[31] from the NIH found that magnetic resonance imaging could localize only 20% of extrahepatic gastrinomas and 43% of hepatic metastases, whereas computed tomography had sensitivities of 45% for extrahepatic tumors and 71% for hepatic metastases in the same group of patients. Magnetic resonance technology is still in a developmental stage at this point, and some believe that with modification and improvement it has the potential to yield better results in imaging of small and extrapancreatic gastrinomas.[32] Although magnetic resonance imaging is currently more expensive and less sensitive than computed tomography, future studies with more powerful magnets, improved software, and different spin echo techniques, pulse repetition rates, or echo delays, and the introduction of oral contrast agents could yield improved results.[32]

INVASIVE PROCEDURES

Arteriography. Arteriography has long been recommended for localizing islet cell tumors because these are often very vascular neoplasms. When modern techniques with digital subtraction, magnification, and biplanar views are used, most islet cell tumors can be localized with this procedure. Broughan et al.[2] found that arteriography accurately localized six of eight (75%) nonfunctioning islet cell tumors, four of six (67%) gastrinomas, and 15 of 29 (52%) insulinomas. Fraker and Norton[3] reported similar results, with arteriography accurately localizing 16 of 19 (84%) insulinomas, 30 of 44 (68%) gastrinomas, and 86% of liver metastases.[3] Fulton et al.[33] successfully localized insulinomas in 21 of 24 (88%) patients with arteriography. Similarly, Thompson et al.[8] identified 13 of the 16 (81%) islet cell tumors in their series with arteriography. Multiple other series have confirmed these excellent results.[9-11] Thus sensitivities of 80% are routinely reported with arteriography for localization of insulinomas, although results are somewhat worse for gastrinomas. Wise et al.,[24] however, report only a 27% sensitivity for arteriography in localizing gastrinomas in 23 patients. In addition to variable tumor vascularity, this technique is likely limited by the same features that limit computed tomography in the localization of gastrinomas (that is, small size and extrapancreatic location). Arteriography, when used together with computed tomography, can detect 95% of patients with hepatic metastases from gastrinomas, and this combination provides the best current information on preoperative tumor staging.[28]

Selective portal venous sampling. Selective transhepatic portal venous sampling is a technique whereby an intrahepatic branch of the portal vein is percutaneously cannulated. By means of the Seldinger technique, a catheter is then threaded through the hepatic branches of the portal vein under fluoroscopic guidance into the splenic and superior mesenteric veins. Blood is sampled from the tributaries draining different areas of the pancreas, and appropriate hormone (for example, insulin, gastrin, somatostatin, pancreatic polypeptide, depending on the diagnosis) concentrations are measured. Increased hormone concentration from one area is a positive study result and regionalizes the tumor to the part of the pancreas drained by that vein. The criterion for a diagnostic "peak" and the degree of localization vary between groups using this procedure,[18, 20, 35] although most seem to agree with Vinik et al.[20] that specific regionalization of the tumor on the basis of the area of highest hormone gradient to one of three regions of the pancreas (tail, body-neck, head-uncinate process) is the most accurate technique.[20] Very favorable results have been reported by several groups. Vinik et al.[20] found a sensitivity of 81% and a specificity of 91% in a series of 32 patients with insulinomas, only 46% of which had been localized by a combination of ultrasonography, computed tomography, and arteriography. Kallio and Suoranta[15] reported four patients with insulinomas with negative arteriograms in whom localization was successfully accomplished with selective portal vein sampling. Fraker and Norton[3] reported successful localization in seven of seven (100%) patients with insulinomas and 11 of 15 (73%) patients with gastrinomas in their series. Roche et al.[19] likewise accurately localized 21 of 22 (95%) insulinomas and 15 of 16 (94%) gastrinomas in a group of patients where arteriography had only located 32% of insulinomas and 13% of gastri-

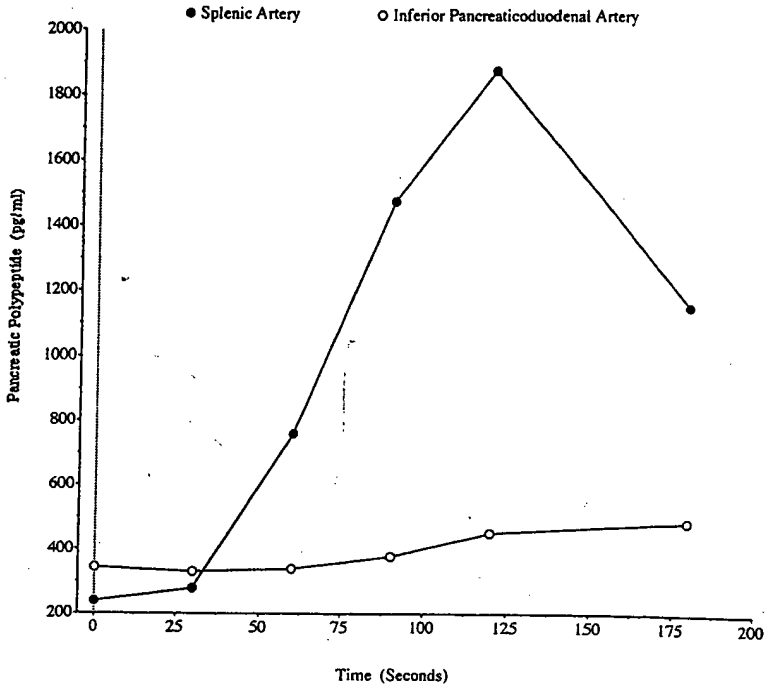

Fig. 1. Results of selective arterial injection of calcium for localization of a pancreatic polypeptide–producing tumor. Injection into the splenic artery causes marked rise in hepatic vein pancreatic polypeptide levels, whereas injection into the inferior pancreaticoduodenal artery causes no change. Tumor was thus regionalized to body-tail of pancreas. Injection of methylene blue into splenic artery provided pinpoint localization of tumor at laparotomy.

nomas. Half the tumors in this series measured less than 15 mm, suggesting that selective portal venous sampling is not as limited by size constraints as are arteriography and computed tomography. Such results have prompted at least one group to advocate routine selective portal venous sampling in all cases of insulinoma.[18]

Although regionalization of tumor with selective portal vein sampling is more sensitive than other preoperative localization studies, the procedure is invasive, expensive, and difficult for both physician and patient. The anatomic variations in pancreatic venous drainage, especially after previous exploration and pancreatic mobilization, may make interpretation of these studies difficult. Also this technique is not sensitive for locating metastases for tumor staging.[19] Given new developments in arteriographic stimulation studies, which will be described herein, we rarely find indication for the performance of selective portal venous sampling at this time.

Selective arterial stimulation testing. Provocative tests have long been used to establish the diagnosis of insulinoma and gastrinoma. Isenberg et al.[36] first documented a paradoxical rise in serum gastrin level after the administration of intravenous secretin, and this has become a standard diagnostic test for Zollinger-Ellison syndrome. Kaplan et al.[37] similarly showed that intravenous calcium can accentuate the elevation of serum insulin levels and depress glucose levels in patients with insulinomas. These provocative tests have recently been combined with the newer radiologic techniques of superselective mesenteric arteriography to develop a new localization test for islet cell tumors. The selective arterial stimulation test with secretin was first proposed by Imamura et al.[38] in 1987 for the localization of gastrinomas. With this technique a catheter is first placed to take blood samples from the hepatic vein. After this is completed, the arteriographic catheter is placed. Before contrast is injected, 30 units of secretin is injected into the splenic, gastroduodenal, and inferior pancreaticoduodenal arteries. Samples are drawn from the hepatic vein at specified time intervals after the injection into each of the individual arteries. The vessel that feeds the tumor can thus be determined based on which secretin injection causes a spike in hepatic vein gastrin concentration. Each injected artery supplies a specific area of the pancreas: the splenic artery supplies the body

Table I. Summary of sensitivities (%) of preoperative localization procedures for islet cell tumors

	Insulinomas					*Gastrinomas*					*Overall*				
Authors	*U/S*	*CT*	*MRI*	*Angio*	*PVS*	*U/S*	*CT*	*MRI*	*Angio*	*PVS*	*U/S*	*CT*	*MRI*	*Angio*	*PVS*
Broughan et al.[2]	0	61	—	52	—	—	67	—	—	—	50	56	—	59	—
Deveney et al.[21]	—	—	—	—	—	—	81	—	—	—	—	81	—	—	—
Fraker and Norton[3]	25	43	—	84	100	20	59	—	68	73	22	55	—	73	82
Frucht et al.[31]	—	—	—	—	—	20	45	20	80	—	20	45	20	80	—
Fulton et al.[10]	—	—	—	88	—	—	—	—	—	—	—	—	—	88	—
Grant et al.[1]	59	36	—	53	—	—	—	—	—	—	59	36	—	53	—
Gunther et al.[7]	—	—	—	—	—	—	—	—	—	—	60	44	—	—	—
Holm et al.[11]	—	24	—	87	—	—	—	—	—	—	—	50	—	64	—
Howard et al.[27]	—	—	—	—	—	—	30	—	—	—	—	30	—	—	—
Katz et al.[16]	—	—	—	43	85	—	—	—	—	—	—	—	—	43	85
Pedrazzoli et al.[18]	—	—	—	—	100	—	—	—	—	—	—	—	—	—	100
Roche et al.[19]	—	—	—	32	95	—	—	—	13	94	—	—	—	24	95
Stark et al.[12]	—	57	—	—	—	—	75	—	—	—	—	64	100	—	—
Thompson et al.[8]	—	—	—	—	—	—	—	—	—	—	72	96	—	81	—
Thompson et al.[22]	—	—	—	—	—	—	—	—	32	25	—	—	—	32	25
Vinik et al.[20]	—	—	—	35	91	—	—	—	—	—	—	—	—	35	91
Wise et al.[24]	—	—	—	—	—	25	29	20	27	—	25	29	20	27	—

U/S, Ultrasonography; *CT*, computed tomography; *MRI*, magnetic resonance imaging; *Angio*, angiography; *PVS*, portal venous sampling.

and tail; the gastroduodenal artery supplies the upper half of the head of the pancreas and duodenum; the inferior pancreaticoduodenal artery supplies the lower half of the head and duodenum. Thus it is possible to determine whether the gastrinoma is in the feeding area of each artery and to regionalize the tumor to one of three areas in the pancreas, much like selective portal venous sampling. In addition to this sensitive regionalization, arteriography is performed as part of this procedure, automatically contributing its valuable localization information.

Imamura et al.[38] successfully used selective arterial secretin injection in four patients with gastrinomas. In three of the patients the tumors were visualized on arteriography and confirmed by selective arterial stimulation testing. In the fourth patient the tumor could not be localized by any other localization tests, including arteriography, but was successfully localized and resected with the aid of selective arterial stimulation testing. Doppman et al.[39] studied 13 consecutive patients with gastrinomas with this technique and documented positive results in five of 13 (38%) by arteriography, seven of 13 (54%) by the selective arterial stimulation testing, and 10 of 13 (77%) with the combination of the two. Both groups believe that this is the most sensitive testing available for gastrinomas. More recently the NIH group has also used this technique with intraarterial calcium as the stimulating agent to successfully localize four consecutive insulinomas that were less than 15 mm.[40] We have recently used a modification of this technique to localize and successfully resect two small islet cell tumors, and we now present our preliminary results.

Selective arterial methylene blue injection. Certain tissues, including islet cell tumors, will stain selectively with intravenously or intraarterially infused vital dyes such as methylene blue.[41-45] We have used this property of islet cell tumors to develop a new localization technique, selective arterial injection of methylene blue. This technique is based on the previously described method of selective arterial stimulation testing. After the feeding artery is localized by the methods described, a catheter is then positioned in the same artery on the morning when laparotomy is to be performed. At operation 2 ml of sterile methylene blue (American Regent Laboratories, Inc., Shirley, N.Y.) is rapidly injected into the catheter. Within 15 seconds the entire area fed by this artery turns blue. The discoloration then clears after 2 minutes except for the islet cell tumor, which in both cases studied thus far has retained the dye for longer than 15 minutes, allowing plenty of time for pinpoint localization and resection. Thus the regionalization provided by the selective arterial stimulation is carried one step further to precise intraoperative localization by the methylene blue injection. Our initial two cases are presented here in detail.

Case 1. A 40-year-old woman presented with persistent Zollinger-Ellison syndrome despite excision of a 2 cm duodenal gastrinoma several months earlier. Results of all localization studies, including ultrasonography, computed tomography, and angiography, were negative. Selective arterial secretin injection and hepatic venous sampling were performed as described by Imamura et al.[38] Superselective arteriography failed to reveal the tumor. The tip of a 5.0F angiographic catheter was inserted sequentially into the gastroduodenal and splenic arteries. Next, serum gastrin levels were obtained from the hepatic vein before and 20, 40, 60, 90, and 120 seconds after 30 units secretin (Ferring Laboratories, Inc., Suffern, N.Y.) was injected selectively into each artery. Serum gastrin concentrations were determined using the Gastrin I^{125} Radioimmunoassay Kit (Becton Dickinson and Co., Orangebury, N.Y.). The feeding artery of the gastrinoma, in this case the gastroduodenal, was identified when the hepatic venous gastrin levels rose more than 800 pg/ml within 40 seconds to at least 120% of the baseline level. On the morning of operation a 5.0F catheter was replaced in the feeding vessel under fluoroscopic guidance. At laparotomy no tumor was evident despite careful operative exploration, intraoperative ultrasonography, and transillumination of the duodenum. Then 2 ml of sterile methylene blue was injected through the prepositioned catheter. Within 15 seconds the entire duodenum and head of the pancreas stained blue. This discoloration cleared after 2 minutes except for a 1 cm area in the second portion of the duodenum, which remained blue for more than 15 minutes. After a longitudinal duodenotomy was performed, a 6 mm stained lesion was easily identified from the normal surrounding mucosa. The tumor was excised and was confirmed by immunohistochemistry to be a gastrinoma. Since the operation the patient has been free of symptoms and has had negative results from a secretin stimulation test.[46]

Case 2. A 72-year-old man with abdominal pain was referred because of a possible mass in the tail of the pancreas found on computed tomography. Serum glucagon and pancreatic polypeptide levels were elevated. The details of the arteriographic procedure are identical to those previously outlined. Arteriography revealed a 2 cm tumor blush in the tail of the pancreas. Stimulation testing was performed in this case with intraarterially injected calcium, as described by Doppman et al.[40] Serum pancreatic polypeptide and glucagon levels from the hepatic vein were obtained before and 30, 60, 90, 120, and 180 seconds after the injection of 5 ml of 10% calcium gluconate (Lymphomed, Rosemont, Ill.) into each artery. Serum pancreatic polypeptide levels were determined by ^{125}I pancreatic polypeptide radioimmunoassay (Mayo Medical Laboratories, Rochester, Minn.). Serum glucagon levels were determined by ^{125}I glucagon radioimmunoassay (SmithKline Beecham, Philadelphia, Pa.). The feeding artery, in this case the splenic, was identified by an increase of 500% in the baseline pancreatic polypeptide level when calcium was injected into it (Fig. 1). No change in glucagon levels occurred. On the morning of operation a 5.0F catheter was replaced in the splenic artery under fluoroscopic guidance. At exploration a mass was evident in the tail of the pancreas. Then 2 ml of sterile methylene blue was injected through the prepositioned catheter. The spleen and entire body and tail of the pancreas stained blue and then cleared after 2 minutes except for the 2 cm nodule in the tail of the pancreas. A distal pancreatectomy was performed, and the mass was confirmed by immunohistochemistry to be rich in pancreatic polypeptide. No evidence of metastasis was present.

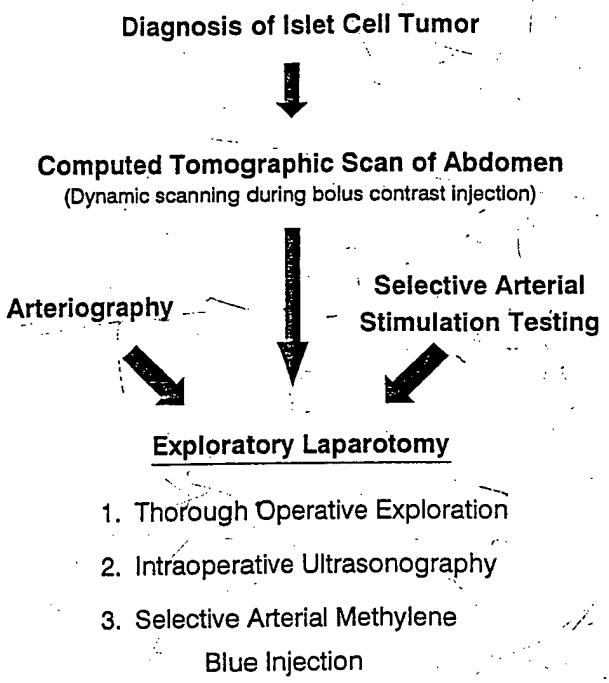

Fig. 2. Currently recommended localization strategy in patients with islet cell tumors of the pancreas.

Intraoperative ultrasonography. Recently intraoperative ultrasonography has been proposed by several authors as a major aid during operative exploration.[1, 47, 48] It is especially helpful in localizing small, deep-seated tumors within the head of the pancreas. Islet cell tumors appear sonolucent and are easy to distinguish from the surrounding pancreatic parenchyma. In addition, it is often possible to ascertain the tumor's relationships to major vessels and the pancreatic and common bile ducts.[49, 50] Intraoperative ultrasonography can also detect features such as indistinct borders that can potentially predict invasiveness and help avoid inappropriate local resections of malignant lesions.[47] In a prospective trial conducted at the NIH comparing palpation with operative ultrasonography, Norton et al.[47] found that palpation was the single best localization modality. Operative ultrasonography and palpation both had more than 90% sensitivities for locating pancreatic gastrinomas, whereas palpation was able to lo-

cate all 12 (100%) of the extrapancreatic gastrinomas, and ultrasonography could locate only seven (58%). Overall, operative ultrasonography had a sensitivity of 85% and affected the decision process in 11% of cases. Grant et al.[1] reported a series of 36 consecutive patients with insulinoma treated at the Mayo Clinic. Intraoperative ultrasonography had a 90% sensitivity for localizing tumors. All 36 underwent successful resection of their insulinomas. These authors propose that a preoperative ultrasonogram combined with intraoperative ultrasonography are sufficient to proceed to initial exploration for insulinomas with good results. Although we cannot support this minimalist approach, we agree that intraoperative ultrasonography is a valuable tool and should be a routine part of the abdominal exploration for islet cell tumors.

Somatostatin-receptor imaging. Some pancreatic endocrine tumors have a large amount of high-affinity somatostatin binding sites.[51] Octreotide, a somatostatin analog, has been labeled with iodine 123 and recently used for localization in nine patients with islet cell tumors. Preoperative localization was performed with gamma scanners. Tumors were successfully localized in seven of nine patients, with tumor sizes ranging from 2 to 14 cm. Both patients in whom the tumor was not localized had insulinomas, neither of which bound labeled octreotide in vitro after tumor resection.[52] This technique may additionally have potential use as an intraoperative localization test that uses a sterile gamma probe at laparotomy to localize the bound somatostatin, although such attempts have not yet been performed.

CONCLUSIONS

Many techniques exist for the localization of islet cell tumors of the pancreas (Table I). Preoperative ultrasonography gives very low yields for accurate localization in most hands and cannot be routinely recommended at all centers. Computed tomography is noninvasive, relatively inexpensive, can localize 50% to 70% of tumors, and aids tumor staging. Therefore we recommend computed tomography as the routine initial localizing procedure once the diagnosis of islet cell tumor is certain. Magnetic resonance imaging is more costly and less sensitive at this time, although magnetic resonance possesses the potential for future improvements in technology that may make it more accurate. Selective portal venous sampling, although it is a sensitive means of regionalizing tumors to an area of the pancreas, is very invasive and difficult to perform. Indications for its use are very limited at this time. Arteriography with selective arterial stimulation provides more information with comparable sensitivity and simpler methodology. Selective arterial injection of methylene blue is a new method for advancing the results of selective arterial stimulation from the level of tumor regionalization to the level of pinpoint intraoperative localization. We feel that patients with the diagnosis of a functioning islet cell tumor should undergo computed tomography scanning followed by arteriography and selective arterial stimulation testing (Fig. 2). A thorough operative exploration must still be considered the best and most important localization procedure. We believe intraoperative ultrasonography is an important adjunct for the surgeon performing that exploration. We shall continue to investigate selective arterial methylene blue injection, because it is an appealing combination of a physiologically based diagnostic procedure, an imaging procedure, and an intraoperative localization procedure.

REFERENCES

1. Grant CS, van Heerden J, Charboneau JW, James EM, Reeding CC. Insulinoma: the value of intraoperative ultrasonography. Arch Surg 1988;123:843-8.
2. Broughan TA, Leslie JD, Soto JM, Hermann RE. Pancreatic islet cell tumors. SURGERY 1986;99:671-8.
3. Fraker DL, Norton JA. Localization and resection of islet cell tumors of the pancreas. JAMA 1988;259:3601-5.
4. Howard TJ, Zinner MJ, Stabile BE, Passaro E. Gastrinoma excision for cure. Ann Surg 1990;211:9-14.
5. Legaspi A, Brennan MF. Management of islet cell carcinoma. SURGERY 1988;104:1018-23.
6. Monténegro F, Lawrence GD, Macon W, Pass C. Metastatic glucagonoma: improvement after surgical debulking. Am J Su... 1980;139:424-7.
7. Gunther KW, Klose KJ, Ruchert K, et al. Islet-cell tumors: detection of small lesions with computed tomography and ultrasound. Radiology 1983;148:485-8.
8. Thompson GB, van Heerden JA, Grant CS, Carney JA, Ilstrup DM. Islet cell carcinomas of the pancreas: a twenty-year experience. SURGERY 1988;104:1011-7.
9. Alfidi RJ, Bhyun DS, Crile G, Hawk W. Arteriography and hypoglycemia. Surg Gynecol Obstet 1971;133:447-52.
10. Fulton RE, Sheedy PF, McIlrath DC, Ferris DO. Preoperative angiographic localization of insulin-producing tumors of the pancreas. AJR 1975;123:367-77.
11. Holm A, Reyes-Govea J, Aldrete JS. Diagnosis, surgical aspects, and long-term followup of functioning and nonfunctioning islet cell tumors of the pancreas. Contemp Surg 1989; 34:13-20.
12. Stark DD, Moss AA, Goldberg HI, et al. Computed tomography and nuclear magnetic resonance imaging of pancreatic islet cell tumors. SURGERY 1983;94:1024-7.
13. Cho KJ, Vinik AI, Thompson NW, et al. Localization of the source of hyperinsulinism: percutaneous transhepatic portal and pancreatic vein catheterization with hormone assay. AJR 1982; 139:237-45.
14. Ingemansson S, Kuhl C, Larsson LI, Lunderquist A, Lundquist I. Localization of insulinomas and islet cell hyperplasias by pancreatic vein catheterization and insulin assay. Surg Gynecol Obstet 1978;146:725-34.

15. Kallio H, Suoranta H. Localization of occult insulin secreting tumors of the pancreas. Ann Surg 1979;189:49-52.
16. Katz LB, Aufses AH, Rayfield E, Mitty H. Preoperative localization and intraoperative glucose monitoring in the management of patients with pancreatic insulinoma. Surg Gynecol Obstet 1986;163:509-12.
17. Norton JA. Resection of islet cell tumors. Contemp Surg 1989;34:57-64.
18. Pedrazzoli S, Feltrin G, Dodi G, et al. Usefulness of transhepatic portal catheterization in the treatment of insulinomas. Br J Surg 1980;67:557-61.
19. Roche A, Raisonnier A, Gillon-Savouret MC. Pancreatic venous sampling and arteriography in localizing insulinomas and gastrinomas: procedure and results in 55 cases. Radiology 1982;145:621-7.
20. Vinik AI, Delbridge L, Moattari R, Cho K, Thompson N. Transhepatic portal vein catheterization for localization of insulinomas: a ten year experience. SURGERY 1991;109:1-11.
21. Deveney CW, Deveney KE, Stark D, et al. Resection of gastrinomas. Ann Surg 1983;198:546-53.
22. Thompson JC, Lewis BG, Wiener I, Townsend CW. The role of surgery in the Zollinger-Ellison syndrome. Ann Surg 1983;197:594-607.
23. Stefanini P, Carboni M, Patrassi N, Basoli A. Beta-islet cell tumors of the pancreas: results of a study of 1067 cases. SURGERY 1974;75:597-609.
24. Wise SR, Johnson J, Sparks J, Carey LC, Ellison EC. Gastrinoma: the predictive value of preoperative localization. SURGERY 1989;106:1087-93.
25. Krudy AG, Doppman JL, Jensen RT, et al. Localization of islet cell tumors by dynamic CT: comparison with plain CT, arteriography, sonography, and venous sampling. AJR 1984;143:585-9.
26. Dunnick NR, Long JA, Krudy A, Shawker TH, Doppman JL. Localizing insulinomas with combined radiographic methods. AJR 1980;135:747-52.
27. Howard TJ, Zinner MJ, Stabile BE, Passaro E. Gastrinoma excision for cure: a prospective analysis. Ann Surg 1990;211:9-14.
28. Norton JA, Doppman JL, Collen MJ, et al. Prospective study of gastrinoma localization and resection in patients with Zollinger-Ellison syndrome. Ann Surg 1986;204:468-79.
29. Prinz RA, Badrinath K, Chejfec G, et al. "Non-functioning" islet cell carcinoma of the pancreas. Am Surg 1983;49:345-9.
30. Eelkema EA, Stephens DH, Ward EM, Sheedy PF. CT features of nonfunctioning islet cell carcinoma. AJR 1984;143:943-8.
31. Frucht H, Doppman JL, Norton JA, et al. Gastrinomas: comparison of MR imaging with CT, angiography, and US. Radiology 1989;171:713-7.
32. Norton JA, Jensen RT. Unresolved surgical issues in the management of patients with Zollinger-Ellison syndrome. World J Surg 1991;15:151-9.
33. Fulton RE, Sheedy PF, McIlrath DC, Ferris DO. Preoperative angiographic localization of insulin-producing tumors of the pancreas. AJR 1975;123:367-77.
34. Stefanini P, Carboni M, Patrassi N, et al. The value of arteriography in the diagnosis and treatment of insulinomas. Am J Surg 1975;131:352-6.
35. Harmon JW, Norton JA, Collin MJ, et al. Removal of gastrinomas for control of Zollinger-Ellison syndrome. Ann Surg 1984;200:396-404.
36. Isenberg JI, Walsh JH, Passaro E. Unusual effect of secretin in a patient with suspected Zollinger-Ellison syndrome. Gastroenterology 1972;62:626-31.
37. Kaplan EL, Rubenstein AH, Evans R, et al. Calcium infusion: a new provocative test for insulinomas. Ann Surg 1979;190:501-7.
38. Imamura M, Takahashi K, Adachi H, et al. Usefulness of selective arterial secretin test for localization of gastrinoma in the Zollinger-Ellison syndrome. Ann Surg 1987;205:230-9.
39. Doppman JL, Miller DL, Chang R, et al. Gastrinomas: localization by means of selective intraarterial injection of secretin. Radiology 1990;174:25-9.
40. Doppman JL, Miller DL, Chang R, et al. Insulinomas: localization with selective intraarterial injection of calcium. Radiology 1991;178:237-41.
41. Hurvitz RJ, Hurvitz JS, Morgenstern L. "In vivo" staining of the parathyroid glands and pancreas. Arch Surg 1967;95:274-7.
42. Keaveny TV, Fitzgerald PA, McMullin JP. Selective parathyroid and pancreatic staining. Br J Surg 1969;56:595-6.
43. Yeager RM, Krementz ET. Toluidine blue in identification of parathyroid glands at operation. Ann Surg 1969;169:829-38.
44. Keaveny TV, Tawes R, Belzer FO. A new method for intraoperative identification of insulinomas. Br J Surg 1971;58:233-4.
45. Gordon DL, Airan MC, Suvanich S. Visual identification of an insulinoma using methylene blue. Br J Surg 1974;61:363-4.
46. Ko TC, Flisak M, Prinz RA. Selective intraarterial methylene blue injection—a novel method of localizing gastrinoma. Gastroenterology 1992;102:1062-4.
47. Norton JA, Cromack DT, Shawker TH, et al. Intraoperative ultrasonographic localization of islet cell tumors: a prospective comparison to palpation. Ann Surg 1988;207:160-8.
48. Sigel B, Coelho JCU, Nyhus LM, et al. Detection of pancreatic tumors by ultrasound during surgery. Arch Surg 1982;117:1058-61.
49. Lane RJ, Coupland GAE. Operative features of insulinomas. Am J Surg 1982;144:585-7.
50. Norton JA, Sigel B, Baker AR, et al. Localization of an occult insulinoma by intraoperative ultrasonography. SURGERY 1985;97:381-4.
51. Reubi JC, Maurer R, von Werder K, Torhorst J, Klijn JG, Lamberts SW. Somatostatin receptors in human endocrine tumors. Cancer Res 1987;47:551-8.
52. Lamberts SWJ, Bakker WH, Reubi JC, Krenning EP. Somatostatin-receptor imaging in the localization of endocrine tumors. N Engl J Med 1990;323:1246-9.

The Laryngoscope
Lippincott–Raven Publishers, Philadelphia

How I Do It

Head and Neck and Plastic Surgery

A Targeted Problem and Its Solution

Intraoperative Use of Methylene Blue to Localize Parathyroid Adenoma

Gregory K. Meekin, MAJ, MD, MC, USAF

INTRODUCTION

Parathyroid surgery for hypercalcemia resulting from adenoma has until recently been somewhat difficult because of a lack of an adequate preoperative study to localize the lesion. Use of ultrasound, computed tomography, nuclear medicine studies, selective venous sampling, selective arteriography, and magnetic resonance imaging scan has been described with varying sensitivities and specificity. More sensitive assays for parathyroid hormone have enhanced the ability to diagnose adenoma, but a good imagining study has been elusive. A technique using methylene blue 7.5 mg/kg intravenously administered approximately 45 minutes to 1 hour before incision allows visualization of the adenoma with greater than 95% sensitivity and specificity. I describe the use of this technique at my institution, reducing surgical time and frustration. This will prove to be a useful localizing study to the parathyroid surgeon and reduce complications.

The search for an ideal localizing technique in parathyroid surgery has been an ongoing process. Preoperative techniques using radionuclide studies, magnetic resonance imaging, computed tomography, ultrasound, selective arteriography, and selective venous sampling for parathyroid hormone have all been reported with varying sensitivities and specificities.[1] In 1966 Klopper and Moe[2] were experimenting with toluidine blue in dogs to define the gastric antrum from the corpus and noted that the pancreas was stained. They also showed that the parathyroid glands stained as well.[2] Hurvitz et al.[3] in 1967 used this knowledge, extended it to humans, and demonstrated successful staining of parathyroids.[3] However, with further use of toluidine, severe cardiac side effects were encountered and its use was abandoned. Dudley[4] in 1971 used methylene blue in 17 patients and demonstrated successful parathyroid staining. Since that time, many reports have followed, primarily in the European literature, describing the use of methylene blue.[5–8]

TECHNIQUE

My colleagues and I have used methylene blue at our institution with great success to localize parathyroid adenomas. All patients are given methylene blue 7.5 mg/kg in 500 mL of normal saline as an intravenous infusion approximately 45 to 60 minutes before incision. The timing is critically regulated to the above schedule.

Adenomas stain dark blue to purple, and normal parathyroid tissue stains less intensely than adenomas. The only negative effect of methylene blue is an alteration in pulse oximetry monitoring during the infusion and at the beginning of cervical exploration. Monitoring returns to normal within 15 minutes after the end of the infusion. Adenomas are confirmed on frozen section. Average duration of exploration to identify adenomas is 7 minutes.

DISCUSSION

Primary hyperparathyroidism is becoming a more recognized disease with increased use of screening calcium levels and better assays for intact parathyroid hormone. With increased recognition, greater numbers of patients are being referred for surgical consideration. Therefore a technique that assists with rapid localization of parathyroid adenomas is useful.

The use of methylene blue has been described previously by several authors, mainly in the European literature.[4–8] Various doses have been used with some concern for potential toxicity. The dose we chose (7.5 mg/kg) has most recently been described as having the best staining

From the Department of Otolaryngology—Head and Neck Surgery, Keesler Medical Center, Keesler Air Force Base, Mississippi.

The opinions and assertions contained herein are the private views of the author and are not to be construed as the official policy or position of the U.S. Government, the Department of Defense, or the Department of the Air Force.

Send Correspondence to Maj. Gregory K. Meekin, MC, USAF, Otolaryngology—Head and Neck Surgery, 81st MG/SGCSL, 301 Fisher Street, Rm/A132, Keesler AFB, MS 39534-2519, U.S.A.

minutes before exploration ensures maximal staining. This certainly is our experience. The staining is dramatic for the adenomas and only light for the normal glands, in contrast to the findings by Gavilan et al.[10] This allows us to rapidly identify the adenoma. The greatest frustration for us is waiting for confirmation of diagnosis on frozen section, which allows us to close the wound. Recently it has been suggested that if an intensely stained adenoma is found, there is no need for biopsy of any other glands.[9] We believe that, if a second gland is visualized with only light staining, this is a reasonable approach, and in the future we will not obtain biopsy specimens of normal glands. However, we will continue to explore the other glands to confirm light staining, as well as to avoid missing the unlikely 4% of cases with a second adenoma.

The surgeon should be aware that during the infusion and for approximately 30 minutes after infusion, pulse oximetry can be erroneously low. This has not been reported before in parathyroid surgery and can result in anesthetic concerns of hypoxia. If any question exists as to the patient's oxygen saturation, a blood gas value can be obtained and oxygenation confirmed. The color of the patient has been described as a pseudocyanosis from the dye; this is a very transient phenomena.[11] The patient's urine will remain intensely stained for a few days. This is the only remaining effect of infusion, and the patient should be alerted to this effect.

Methemoglobinemia has been a potential concern. My colleagues and I measured the blood level of methemoglobin in our first patient and found it to be insignificant. Devine et al.[12] measured levels in five patients, using a dose of methylene blue of 5 mg/kg, and found them to be insignificant as well. Although a theoretical concern, in several hundred patients no symptomatic methemoglobinemia has been described in the literature. Pain at the infusion site has been reported sporadically, but our patients have not experienced this. We have been very satisfied that methylene blue at 7.5 mg/kg is a safe and effective dose.

Attempts have been made to use radiolabeling with methylene blue, as well as other thiazide dyes (toluidine blue, thioinine); however, success has been limited.[13] If this could be perfected, perhaps a more accurate preoperative imaging study will be available in the future.

Methylene blue has also been used to locate normal and hyperplastic parathyroid glands. This can prove useful in thyroid cancer surgery and in renal failure with secondary hyperparathyroidism.[14] The mechanism of glandular uptake is unknown. One report described the staining mainly in the oxyphil cells, not the chief cells, which are thought to be responsible for parathyroid hormone production.[15] The significance of this finding is uncertain.

CONCLUSION

My colleagues and I have found methylene blue to be very helpful in identifying parathyroid adenomas. It is safe, reliable, and consistent. Other techniques for preoperative localization have varying results and in our experience have not been useful. Methylene blue is easy and cost-effective, resulting in fast localization and reduced surgical time for resection of parathyroid adenomas.

BIBLIOGRAPHY

1. Potchen JE. Editorial parathyroid imaging: current status and future prospects. *J Nucl Med* 1992;33(10):1807–9.
2. Klopper PJ, Moe RE. Demonstration of the parathyroids during surgery in dogs, with preliminary report of results in some clinical cases. *Surgery* 1966;59:1101–7.
3. Hurvitz RJ, Perzik SL, Morgenstern L. In Vivo staining of the parathyroid glands: a clinical study. *Arch Surg* 1968;97: 722–6.
4. Dudley NE. Methylene blue for rapid identification of the parathyroids. *Br J Med* 1971;3:680–1.
5. Gordon DL, Airan MC, Thomas W, et al. Parathyroid identification by methylene blue infusion. *Br J Surg* 1975;62: 747–9.
6. Bambach CP, Reeve TS. Parathyroid Identification by methylene blue infusion. *Aust N Z J Surg* 1978;48(3):314–7.
7. Sherlock DJ, Holl-Allen RTJ. Intravital methylene blue staining of parathyroid glands and tumours. *Ann R Coll Surg Engl* 1984;66:396–8.
8. Derom A, Wallaert P, Janzing H, et al. Intraoperative identification of parathyroids by means of methylene blue. *Acta Chir Belg* 1994;94:97–100.
9. Derom AF, Wallaert PC, Heinrich MJ, et al. Intraoperative identification of parathyroid glands with methylene blue infusion. *Am J Surg* 1993;165:380–2.
10. Gavilan J, Gavilan C, Tomas MD. Methylene blue infusion for intraoperative identification of the parathyroid glands. *Laryngoscope* 1986;96:1389–90.
11. Wheeler MH, Wade JHS. Intraoperative identification of parathyroid glands: appraisal of methylene blue staining. *Am J Surg* 1982;143:713–6.
12. Devine RM, van Heerden JA, Grant CS, et al. The role of methylene blue infusion in the management of persistent or recurrent hyperparathyroidism. *Surgery* 1983;4:916–8.
13. Blower PJ, Kettle AG, O'Doherty MJ, et al. 123 I–Methylene blue: an unsatisfactory parathyroid imaging agent. *Nucl Med Commun* 1992;13:522–7.
14. Bland KI, Tidwell S, von Fraunhofer JA, et al. Intraoperative localization of parathyroid glands using methylothionine chloride tetramethylthionine chloride in secondary hyperparathyroidism. *Surg Gynecol Obstet* 1985;160:42–8.
15. Lavelle MA. Parathyroid adenoma stained with methylene blue. *J R Soc Med* 1980;73:462–3.

Pergamon

Bioorganic & Medicinal Chemistry Letters 11 (2001) 2193–2195

BIOORGANIC & MEDICINAL CHEMISTRY LETTERS

Anticancer Properties for 4,4′-Dihydroxybenzophenone-2,4-dinitrophenylhydrazone (A-007)/3,7-Diaminophenothiazin-5-ium Double Salts

Lee Roy Morgan,[a,*] Andrew H. Rodgers,[a] Blaise W. LeBlanc,[a] Steven M. Boué,[b] Ying Yang,[b] Branko S. Jursic[b] and Richard B. Cole[b]

[a]*DEKK-TEC, Inc., New Orleans, LA 70119, USA*
[b]*The Department of Chemistry, University of New Orleans, New Orleans, LA 70122, USA*

Received 5 February 2001; accepted 7 June 2001

Abstract—4,4′-Dihydroxybenzophenone-2,4-dinitrophenylhydrazone (A-007) formed stable double salts with phenothiazin-5-ium salts (**2a–d**), which have improved in vitro anticancer activities, as compared to A-007 alone. The stable salt between methylene blue (**2a**) and A-007 allowed the latter to diffuse into the dermis layers of skin. It is anticipated that these new salts will allow A-007 to penetrate into the deep lymphatic/vascular channels of the dermis, which contain metastatic cancer cells, and improve in vivo anticancer activities. © 2001 Elsevier Science Ltd. All rights reserved.

4,4′-Dihydroxybenzophenone-2,4-dinitrophenylhydrazone (A-007), **1**, has anticancer activities in vitro and in vivo when applied topically to metastatic cancer spread to the skin.[1–4] Metastatic cancer to the skin does not respond well to systemic therapy.[3] This communication describes the formation of stable double salts between A-007 and sulfur containing π-electron delocalized cationic (EDC) salts that, (1) improved A-007's anticancer activities, and (2) increased A-007's penetration into the dermis (Fig. 1).

Methylene blue (**2a**) and other phenothiazin-5-ium salts (**2b–d**) exist as π-electron deficient species due to sulfur's ability to utilize 3*d* orbitals (a characteristic of 3rd periodic level elements).[5–7] The orbital dynamics of the phenothiazin-5-ium salts have been utilized to produce stable salts with A-007 (Table 1).[8] Some chemistry and biological properties of these double salts are reported in this communication.

A-007 (63 mmol) in 10 mL of ethanol (need to heat to dissolve) was added, with stirring, to 63 mmol of **2a–e**, each dissolved in 10–15 mL of ethanol, and stirred at 75 °C for an additional 15–30 min. The solutions were allowed to stand at refrigerator temperatures overnight. The resulting precipitates (A-007/**2a–d**) were recrystallized from ethanol with 73–100% yield.[9] See Table 1 for structure compositions. All products analyzed correctly as a double salt (A-007/**2a–d**).

Fresh human cancers obtained at surgery, were minced and suspended in 16 mL of RPMI-1640 containing 10% FBS, 10 mg/mL neomycin, 5 mg/mL streptomycin and 5000 U/mL penicillin. The Cytostat® assay was used to determine in vitro anticancer activity for the double salts.[3] A-007 and salts were dissolved in DMSO (5 mg/mL) and used as a stock solution. Doxorubicin (DOX) (Table 1) and the respective base dyes were used as controls. The cultures were exposed to varying

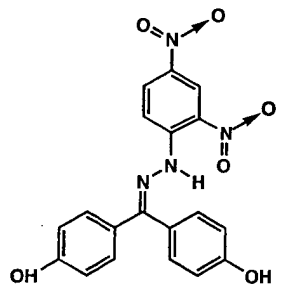

Figure 1. A-007.

*Corresponding author. Fax: +1-504-488-4451; e-mail: lrm1579@aol.com

0960-894X/01/$ - see front matter
PII: S0960-894X(01)00408-5

concentrations of A-007 salts for 72 h, then assayed for cytotoxicity.[3]

In triplicate, dermatomed (0.3–0.4 mm) skin samples from hairless rats were cut into multiple sections large enough to fit on 0.9 cm^2 Franz diffusion chambers. The dermal chambers consisted of 5% BSA in Hepes buffered Hank's balanced salt solution open to the ambient laboratory environment. The Franz diffusion chambers were placed in a diffusion apparatus and the dermal receptor solution stirred at 600 rpm and 32 °C.[10]

The test formulations were applied to triplicate skin sections as a 0.25% propylene glycol gel.[10] At timed intervals, the receptor solution was removed and stored at −70 °C until assayed for A-007. Standard H&E histological examinations were conducted on all treated and control skin specimens upon terminating each study. Quantitation of A-007 was determined by reverse-phase HPLC.[11]

A-007 formed double salts with 3,7-bis(dimethylamino)-phenothiazin-5-ium chloride (methylene blue or MEB, **2a**), 3-amino-7-dimethylamino-2-methylphenothiazin-5-ium chloride (toluidine blue or TB, **2b**), 3,7-bis(dimethylamino)-4-nitrophenothiazin-5-ium chloride (methylene green or MEG, **2c**), and 3,7-bis(diamino)-phenothiazin-5-ium acetate (Thionin or TN, **2d**), while phenothiazine (PT, **2e**) did not react with A-007. The latter observation may be associated with **2e** being unsubstituted (i.e., no –NH, etc.) and unable to stabilize through an EDC resonance, similar to what can exist for **2a–d.**

Table 1. Phenothiazin-5-ium salts

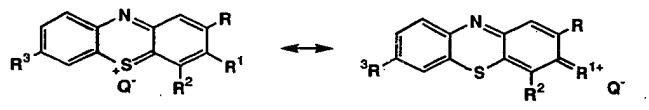

Dyes	R	R^1	R^2	R^3
2a Methylene blue (MEB)	H	$N(CH_3)_2$	H	$N(CH_3)_2$
2b Toluidine blue (TB)	CH_3	NH_2	H	$N(CH_3)_2$
2c Methylene green (MEG)	H	$N(CH_3)_2$	H	$N(CH_3)_2$
2d Thionin (TN)	H	NH_2	H	NH_2
2e Phenothiazine (PT)	H	H	H	H

$Q^- = Cl^-$ or acetate.

Anticancer activities for the A-007 double salts (**2a–d**) in a human cancer tissue explant culture assays are summarized in Table 2. The anticancer activities for the salts are significantly improved when compared to A-007 alone. The activities noted for breast, melanoma and lung are very encouraging. The base dyes (**2a–d**), alone, were not active ($IC_{50} > 30$ mcg/mL); NT = not tested. A-007/MEB and A-007 were tested against normal human peripheral blood dendritic cells and the IC_{50} were calculated to be > 10 mcg/mL.[12]

MEB improved A-007's penetration into tissue and the latter's ability to diffuse through the epidermis and enter channel networks draining the dermis (Table 2). This data supports the concept that π-electron deficient cations (EDC) may be able to deliver A-007 to lymphatic channels/spaces in tissues and thus increase anticancer activities. Histological examinations of the treated skin preparations from Table 3 revealed that A-007/MEB improved A-007's penetration into the dermis, when compared to A-007 alone, which only penetrated the epidermis. A-007 is deep red in color and stains tissues yellow; this property renders it easy to trace.

The above salts do not form acceptable crystals for X-ray crystallography analysis. In an attempt to appreciate the interactions between A-007 and the dyes, ^{15}N-A-007 was synthesized from $(^{15}N)_2$-2,4-DNPH and 4,4-dihydroxybenzophenone.[12] ^{15}N NMR studies failed to reveal an interaction between MEB and A-007's –NH moieties (**2a**). Comparative ^{13}C NMR spectroscopy did not demonstrate any π–π stacking for the **2a**/A-007 salt. No shifts in hydrogen were seen with comparative ^1H NMR spectroscopy for **2a**. In contrast, for the **2d** salt, a broad singlet at 3.6 ppm was observed with ^1H NMR spectroscopy while the phenolic protons of A-007 were absent; this could represent interactions between NH– and HO–. The latter shifts observed with **2d** are probably a result of the reduced bulkiness at the 3- and 7-

Table 2. Comparative IC_{50} sensitivities for primary human cancer culture

Tissue	No.	A-007 (mcg/mL)	A-007/MEB (mcg/mL)	A-007/MEG (mcg/mL)	A-007/TB (mcg/mL)	A-007/TN (mcg/mL)	DOX (mcg/mL)
Breast cancer	4	3≥10	0.3–2.5	NT	0.9–1.5	0.9	0.3–0.9
Melanoma	6	7≥10	0.5–1	0.03–0.4	0.7–4.0	NT	2≥5
Ovarian cancer	3	9	2	NT	NT	0.2	NT
Lung cancer (NSCLC)	4	4	1–2	0.75–1	3	>10	>30

Table 3. Percutaneous absorption in the Franz cell (A-007 vs A-007/MEB diffusion into rat skin)

Test material	Franz chamber (No.)	0.25% Gel applied (mg)	Actual A-007 applied (mg)	A-007 in receptor fluid (ng/mL)
A-007	12	17–56	0.04–0.14	None detected
A-007/MEB	3	14.6	0.05	9

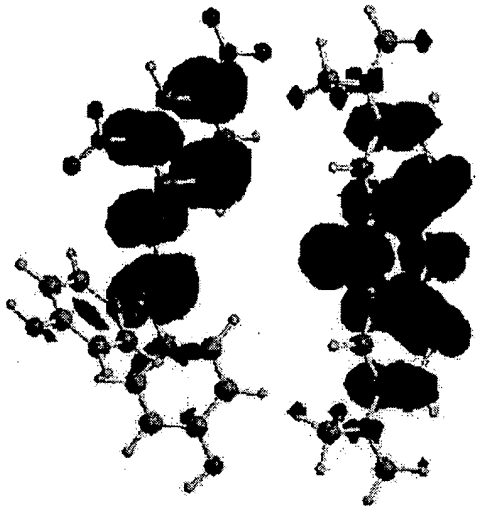

Figure 2. An AM1 generated HOMO–LUMO orbital presentation for A-007 (left) and methylene blue (right).

positions (primary amines) and the close proximity that could occur between A-007's –HOs and **2d**'s –NHs. Based on elemental analysis, IR stretching and NMR singlet shifts noted, the stability of the salts are possibly a result of interactions between the cationic sulfur and the anionic –NH of A-007, as well as the –OHs in A-007 and the 3- and 7-NHs groups in the phenothiazin-5-ium salts. An AM1 semi-empirical method generated a HOMO–LUMO orbital presentation for the A-007/MEB salt that revealed complimentary electronic derivatives that allow a stable configuration to exist (Fig. 2). At least one of A-007's aryl–OHs is required for salt formation.[12]

The described A-007 salts are stable, however, in the presence of tissue highly charged biopolymers and so on, the former are capable of dissociating, releasing A-007 (Table 2). Thus we have successfully generated products that both protect A-007 from non-selective tissue binding, as well as enhance its diffusion into avascular dermal structures that can harbor cancer cells.

Acknowledgements

This work was supported by grant CA 89,772 from the NCI/SBIR FLAIR program.

References and Notes

1. Thangaraj, K.; Morgan, L. R.; Benes, E.; Jursic, B. S.; Fan, D. *Breast Cancer Res. Treat.* **1993**, *27*, 150.
2. Eilender, D. E.; LoRusso, P.; Krementz, E. T.; Tornyos, K.; Thomas, L.; McCormick, C. *Abstract of Papers*, 10th Symposium on New Drugs in Cancer Therapy; NCI/EORTC: Amsterdam, 1998; Abstract 124
3. Morgan, L. R.; Rodgers, A. H.; Fan, D.; Soike, K.; Ratterree, M.; Sartin, B. W.; Harrison, T. J. *In Vivo* **1997**, *11*, 29.
4. Easmon, J.; Heinisch, G.; Purstinger, G.; Hofmann, J. In *Proc. Amer. Assoc. Cancer Res.*, American Association for Cancer Research: San Francisco, CA, 2000; Vol. 41, p 656.
5. Wald, G. In *Horizons in Biochemistry*; Kasha, M., Pullman, B., Eds.; Academic: New York, 1962; pp 127–142.
6. Pullman, B.; Pullman, A. *Biochem. Biophys. Acta* **1959**, *35*, 535.
7. Karreman, G.; Isenberg, I.; Szent-Gyorgyi, A. *Science* **1959**, *130*, 1191.
8. Orloff, M. K.; Fitts, D. D. *Biochem. Biophys. Acta* **1961**, *47*, 596.
9. File: L.R.M.-1579; Protein Data Bank, Brookhaven National Laboratory: Upton, New York.
10. Morgan, L. R.; Rodgers, A. H.; Schwartz, S.; Bies, R.; Krementz, E. T. *Proc. Amer. Assoc. Cancer Res.*; American Association for Cancer Research: New Orleans, LA, 1998; Abstract 597, p 39.
11. Rodgers, A. H.; Subramanian, S.; Morgan, L. R. *J. Chromatogr. B* **1995**, *670*, 565.
12. Morgan, L. R.; Thangaraj, K.; LeBlanc, B. W.; Rodgers, A. H.; Boue', S. M.; Cole, R. B. In *Proc. Mol. Target Cancer Ther.*; AACR/EORTC: Washington, DC, 1999; Abstract 558.

ELSEVIER

Cancer Letters 151 (2000) 161–167

CANCER Letters

www.elsevier.com/locate/canlet

Methylene blue reverts multidrug resistance: sensitivity of multidrug resistant cells to this dye and its photodynamic action

G.S. Trindade[a,b,c], S.L.A. Farias[b], V.M. Rumjanek[c], M.A.M Capella[b,*]

[a]*Departamento de Ciências Fisiológicas, FURG, Rio Grande, RS, Brazil*

[b]*Laboratório de Fisiologia Renal, Instituto de Biofísica Carlos Chagas Filho, Universidade Federal do Rio de Janeiro, CCS, Bloco G, 21949-900 Rio de Janeiro, RJ, Brazil*

[c]*Laboratório de Imunologia Tumoral, Departamento de Bioquímica Médica, Instituto de Ciências Biomédicas, CCS, Universidade Federal do Rio de Janeiro, Rio de Janeiro, RJ, Brazil*

Received 25 June 1999; received in revised form 29 October 1999; accepted 5 November 1999

Abstract

Photodynamic action has been advocated as an alternative treatment of tumors but the most common used dyes, hematoporphyrin derivatives, are substrate for P-glycoprotein. This study investigated the MDR-reverting properties of methylene blue (MB) and compared the sensitivity to its photodynamic action (PDA) in five cell lines that either express or do not express the MDR phenotype. MB was able to revert the MDR phenotype and there was no difference in sensitivity to MB-PDA between MDR and non-MDR cells, suggesting that MB has the advantage of being used simultaneously as a MDR reverser and a photodynamic agent.

Keywords: Multidrug resistance; P-glycoprotein; Methylene blue; Photodynamic action

1. Introduction

Photodynamic action (PDA) is the photooxidation of biological molecules in the presence of oxygen and a sensitizing substance. The inactivation of viruses, bacteria and tumor cells by photodynamic action is of interest because of its potential use in cancer therapy and in the sterilization of blood and plasma concentrates [1–4]. One of the sensitizers under study is methylene blue (MB) [5–11], the photodynamic action (MB-PDA) of which depends on at least three factors: the concentration of the dye, the concentration of O_2, and the intensity of the light. Several mechanisms may be involved in MB-PDA, including the generation of singlet oxygen and direct interaction of MB with cellular targets [3,12,13], leading to oxidative DNA damage, such as guanine oxidation and DNA single-strand breaks [13,14].

Treatment of multidrug resistant (MDR) tumors refractory to conventional chemotherapy is one of the major concerns of oncologists because these tumors need additional drugs to revert the MDR phenotype. The best understood mechanism of MDR is the one conferred by the membrane P-glycoprotein (Pgp), which acts by pumping a number of unrelated drugs from the cells [15]. Much effort has been expended to circumvent this problem, and one of the most promising approaches is the use of Pgp modulators, such as verapamil [16], cyclosporin A [17], or trifluoperazine [18], a phenothiazine that acts as a calmodulin antagonist. Other phenothiazines, such

* Corresponding author. Fax: +55-21-280-8193.
E-mail address: mcapella@biof.ufrj.br (M.A.M. Capella)

0304-3835/00/$ - see front matter
PII: S0304-3835(99)00408-5

as prochlorperazine and fluphenazine, that share some structural features, possess significant activity in reverting the MDR phenotype [19].

Methylene blue is a phenothiazine with strong photodynamic properties that has been shown to be retained in malignant tissues [20–22]. Thus, it would be interesting to establish the possible MDR-reverting properties of MB and the susceptibility of multidrug resistant cells to the MB-PDA. The objectives of this work were to study the use of this dye as a modulator of MDR and to compare the sensitivity to MB-PDA in five cell lines, some of which express the MDR phenotype.

2. Materials and methods

2.1. Cells and culture conditions

MA104 is a constitutive multidrug resistant (MDR^+) cell line derived from Rhesus monkey kidney and overexpressing Pgp [23]. MDCK is a cell line derived from canine kidney that does not present MDR phenotype (MDR^-), although it expresses low amounts of Pgp [24].

The MDCK/60 cell line was derived from MDCK, following the method of Tsuruo et al. [25]. Briefly, the cells were cultured in the presence of progressively higher concentrations of vincristine (VCR), until cells were maintained in the presence of 60 nM of the drug (about six times the lethal dose for the parental MDCK cell line). The cells present characteristics of multidrug resistance, such as alterations in the actin cytoskeleton [26,27] and extrusion of rhodamine 123 ([28] and data not shown).

K562 is an erythroleukemic cell line that does not express the MDR phenotype (MDR^-) and K562-Lucena 1 (Lucena 1) is a MDR^+ cell line obtained from K562 by Rumjanek et al. [29] that expresses characteristics of multidrug resistance due to overexpression of Pgp [23,26].

All the cells were grown in DMEM with 20 mM HEPES and 10% fetal bovine serum, in disposable plastic bottles at 37°C. K562 and Lucena 1 cells were grown in suspension and the three kidney cell lines adhered to the plastic bottles. MDCK/60 and Lucena 1 cells were grown regularly in medium containing 60 nM of VCR. MA104 cells, due to their constitutive MDR phenotype, were grown with VCR (60–90 nM) only during the experiments related to reversion of MDR phenotype.

The growth of all MDR^+ cell lines was delayed in relation to the MDR^-. Thus, the MDR^- cells were passaged 48 h and the MDR^+ cells 72 h before the experiments, to insure that all cell lines were in exponential growth phase at the time of the experiments.

2.2. Cellular toxicity of MB

In order to study the intrinsic cellular toxicity of MB, the cells were harvested (K562 and Lucena 1 by centrifugation and the kidney adherent cells by using trypsin–EDTA) and seeded on 24-well chambers, at a concentration of 1×10^5 cells/ml (2 ml/well), with various concentrations of MB. The cells were then incubated for 48 h at 37°C and at the end of this period the cell number and viability were measured by Trypan Blue exclusion.

2.3. Reversion of the MDR phenotype by MB

To verify if MB acts as a MDR modulator, cultured cells were harvested as described above and incubated in fresh medium with VCR in presence or absence of different concentrations of MB for 48 h at 37°C. The cell number and viability (measured by Trypan Blue exclusion) were evaluated after 48 h of incubation.

2.4. Photodynamic action of methylene blue

To study the photodynamic action of MB, the three kidney cell lines were plated at a concentration of 1×10^5 cell/ml (1 ml/well) in 30-mm dishes and incubated for 16 h to complete cell adhesion. The kidney and erythroleukemia cell lines were then washed twice with phosphate-buffered saline (PBS) and the concentration of the erythroleukemia cells adjusted to 1×10^5 cell/ml. The cells were incubated with various concentrations of the dye for 30 min (in PBS) and illuminated with visible light for 5 min. The light source was a Sylvania flood 'cool-lux' (150 W, 120 V) lamp, with an emission spectrum almost totally in the visible region and a peak of emission in 590 nm. To avoid temperature rises in the illumination chambers, it was employed the same experimental design used previously [5,6,30]. Briefly, a Pyrex receptacle containing distilled

water (2-cm path) was interposed between the lamp and the cells to eliminate heating due to infrared rays. The temperature was monitored and did not rise during the experiments. The illumination was performed at room temperature (approximately 25°C). The distance between the lamp and the dishes containing the cells was 13 cm and the dose rate was 1.5×10^3 W/m^2, as measured by a model 65 A radiometer (Yellow Springs Instrument Co.). This dose was the same as used previously [5,6,30]. After the illumination, the cells were washed twice with PBS, suspended in fresh MB-free medium and incubated at 37°C for 48 h. The cell number and viability were evaluated by Trypan Blue exclusion.

2.5. Statistical analysis

Data obtained were from at least three experiments. The data were analyzed by one-way analysis of variance (ANOVA), considering the treatments as factors. The significance of the differences was verified by the Bonferroni *t*-tests [31].

3. Results

3.1. Cellular toxicity of MB

Fig. 1 shows the sensitivity of the five cell lines to MB. All the MB concentrations used were able to inhibit cell growth, and the toxicity of this dye was dose-dependent, as can be observed by the increased number of Trypan Blue-stained erythroleukemia cells with increased concentrations of MB (Fig. 1A,B) and by a corresponding decrease in the total number of kidney cells, due to cell lysis (Fig. 1C–E).

The erythroleukemia cells (Fig. 1A,B) were more resistant to the toxic effect of MB than the renal cells (Fig. 1C–E). For example, a MB concentration of 1.0 μg/ml led to approximately 20% of viable cells, in comparison to the control, for the three kidney cell lines (Fig. 1C–E) whereas concentrations 6–8 times greater were needed to achieve about the same percentage for the leukemic cells (Fig. 1A,B). However, cells from same origin were equally sensitive to MB, regardless of their MDR phenotype.

3.2. MB partially reverts the MDR phenotype

To verify whether MB acts as a reverser of the MDR phenotype, Lucena-1 cells were incubated with 60 nM VCR, a concentration in which they grow normally, in the presence of different MB concentrations. The graph presented in Fig. 2 shows the viability of Lucena-1 cells incubated with MB + VCR normalized to the viability of Lucena-1 cells incubated with MB alone. It can be seen that MB concentrations of 1 and 2 μg/ml were able to revert partially the resistance of Lucena-1 cells to VCR ($P < 0.05$). Increased concentrations of MB did not lead to significant increase in the reversion, probably due to cellular toxicity. The same treatment was performed for MA104 and MDCK/60 cells, using VCR concentrations to which the cells are resistant (90 and 60 nM, respectively). However, due to their great sensitivity to MB, they were incubated with only 0.5 μg/ml of MB. In Fig. 3 is shown the percentage of viability of MA104 and MDCK/60 cells treated with VCR alone, MB alone or MB + VCR, normalized in relation to the control (cells incubated in medium without any drug). The viability of both cell lines treated only with VCR is 100%, i.e. equal to the control. Methylene blue alone, as expected, is toxic to the cells, and it seems that MA104 cells, with a viability of 30.6 ± 2.7% of the control, are more sensitive to this MB concentration than MDCK/60 cells, that had a viability of 64.1 ± 8.4% of the control ($P < 0.05$). However, when the cells were incubated with VCR + MB, the viabilities of MA104 and MDCK/60 cells decreased to 20.1 ± 1.8 and 42.5 ± 6.2% of the respective controls. These values are statistically different from that obtained for the incubation with MB alone or VCR alone ($P < 0.05$), suggesting that MB reverted partially the resistance of these cells to VCR.

3.3. Cellular sensitivity to MB-PDA

The viability of the five cell lines after 48 h of incubation following photodynamic treatment is shown in Fig. 4. Under the experimental conditions used, the cell number and cell viability did not significantly change immediately after illumination. Furthermore, exposure to light alone or a 30 min incu-

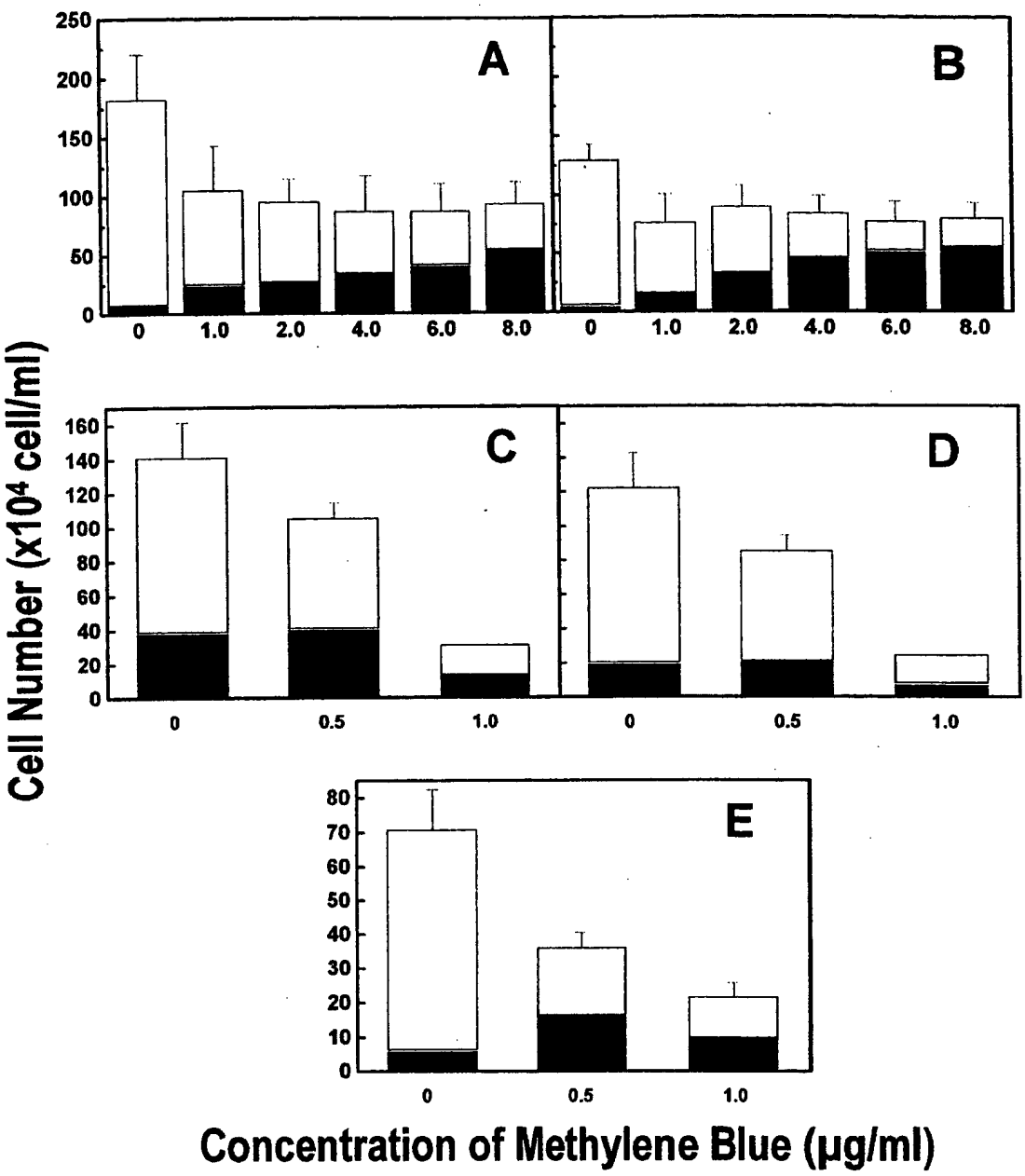

Fig. 1. MB-induced cytotoxicity in erythroleukemia and kidney cells either expressing or not expressing the MDR phenotype. Cells were incubated with MB for 48 h and the cell number and viability was evaluated by Trypan Blue exclusion. Results are expressed as the total cell number (mean ± SD) and in black is the number of cells stained by Trypan Blue. A, K562 cells; B, Lucena-1 cells; C, MDCK cells; D, MDCK/60 cells and E, MA104 cells.

bation with MB alone (4 μg/ml for erythroleukemic cells and 0.5 μg/ml for kidney cells) did not alter cell growth and viability (data not shown). However, 48 h of incubation, in a MB-free medium, following photodynamic treatment considerably decreased the viability of all the cell lines ($P < 0.05$). The figure suggests that K562 and Lucena-1 cells are more sensitive to MB-PDA than kidney cells, but it must be considered

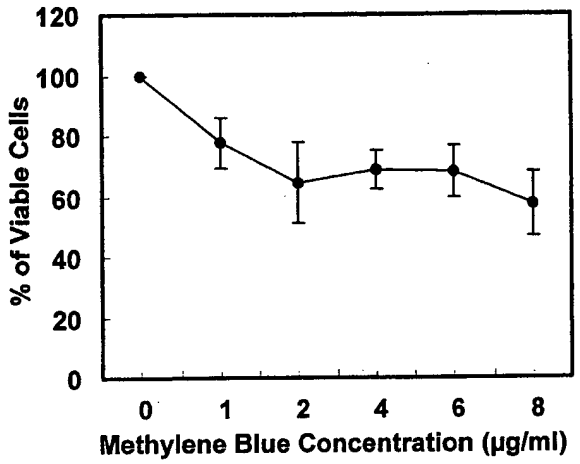

Fig. 2. Reversion of the MDR phenotype by MB. Lucena-1 cells were incubated for 48 h with VCR 60 nM in the presence of various concentrations of MB. The results are expressed as the percentage of cellular viability obtained in the presence of MB + VCR normalized to the cellular viability obtained with MB alone.

that, due to the high sensitivity of kidney cells to MB, a concentration eight times lower (0.5 μg/ml) than that used for the erythroleukemic lines (4 μg/ml) was employed on kidney cells. This may have considerably diminished the photodynamic effect. It can also be seen that the cellular sensitivity to MB-PDA is independent of the MDR phenotype, and in fact the MDR kidney cell lines (MA104 and MDCK/60) were apparently more sensitive to this treatment than the non-MDR one (MDCK).

4. Discussion

The photodynamic action of hematoporphyrin derivatives (HPD) has been advocated as an alternative treatment for MDR tumors [32]. However, it has been shown that these dyes are substrates for P-glycoprotein and that the use of Pgp modulators is necessary in order to obtain good results with this treatment [33].

Methylene blue has been used experimentally with a number of tumors, including in human, either for targeted radiotherapy of melanomas [21] or for treatment of tumors by photodynamic action [7,10,11]. In the present study we showed that the cellular sensitivity to MB and MB-PDA are dependent on the cell origin rather than the MDR phenotype. In accordance to our results, Schick et al. [34] showed that MB-PDA had comparable effects in normal human keratinocytes, spontaneously transformed human keratinocytes and squamous cell carcinoma. Moreover, the cellular toxicity of MB observed in kidney cells was similar to that obtained by Lee and Wurster [35] in human brain tumor cells. Thus, it seems that the erythroleukemia cell lines used in the present study are much more resistant to this dye than other cell lines. Our results showed that, although the erythroleukemia cells are clearly more resistant to MB and MB-PDA than kidney cells, there is no difference in sensitivity between MDR and non-MDR cells from same origin. Moreover, MA104 cells, which express Pgp constitutively [23], are nearly as sensitive to MB and MB-PDA as MDCK/60 cells, suggesting that the

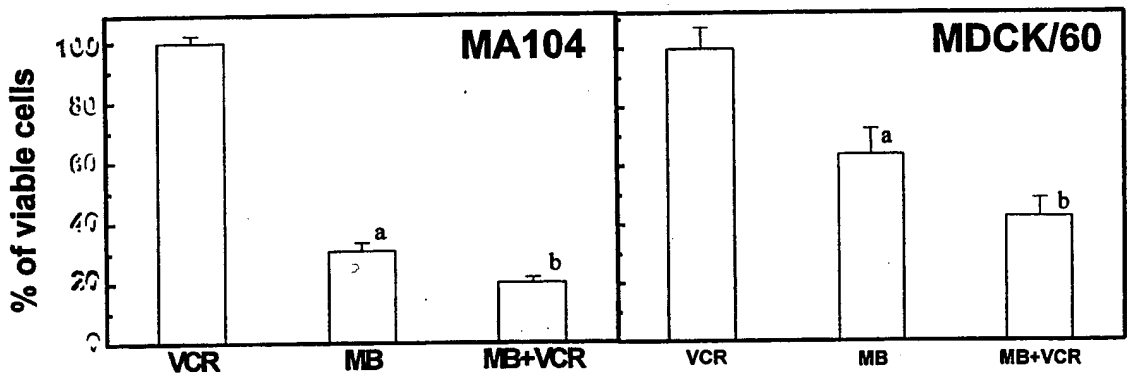

Fig. 3. Reversion of the MDR phenotype of MA104 and MDCK/60 by MB. Cells were incubated for 48 h with VCR (90 nM for MA104 and 60 nM for MDCK/60) in the presence or absence of MB 0.5 μg/ml. The results shown are normalized to the cellular viability presented by the control cells (incubated in medium without any drug). a, Significantly different from VCR; b, significantly different from VCR or MB.

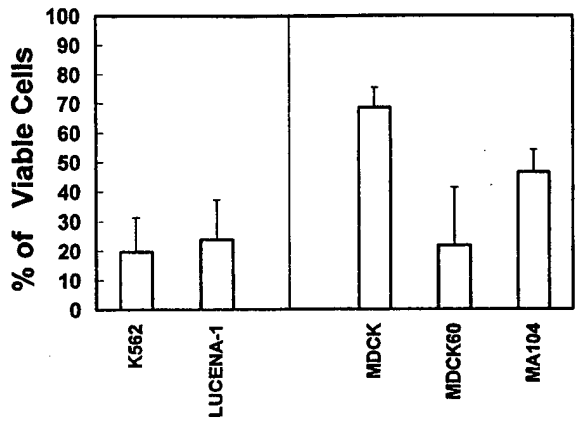

Fig. 4. Viability of erythroleukemia and kidney cells treated with MB-PDA. Cells were incubated with 4.0 μg/ml (erythroleukemia cells) or 0.5 μg/ml (kidney cells) for 30 min, illuminated for 5 min and incubated in MB-free medium for 48 h. Results are expressed as the percentage of viable cells treated with MB-PDA in relation to the control, untreated cells. The viability of cells treated with light alone or MB alone did not differ from the control.

way cells are MDR (constitutively or induced) does not determine their sensitivity to MB and its PDA.

Finally, it was also observed in the present study that MB, rather than being a substrate for Pgp, as hematoporphyrin derivatives, is a MDR reverser. The reversing effect of MB is not as good as the classical Pgp reversers verapamil [16] and cyclosporin A [17], but it has the advantage of being an agent that could be used simultaneously as a MDR reverser and a photodynamic agent.

Acknowledgements

The present work was supported by grants from Conselho Nacional de Pesquisa (CNPq), Capacitação de Pessoal de Ensino Superior (CAPES) and Programa de Apoio aos Núcleos de Excelência (PRONEX).

References

[1] K. Miller-Breitkreutz, H. Mohr, Hepatitis C and human immunodeficiency virus RNA degradation by methylene blue/light treatment of human plasma, J. Med. Virol. 56 (1998) 239–245.
[2] R. Santus, P. Grellier, J. Schrevel, J.C. Maziere, J.F. Stoltz, Photodecontamination of blood components: advantages and drawbacks, Clin. Hemorheol. Microcirc. 18 (1998) 299–308.
[3] M. Ochsner, Photophysical and phobiological processes in the photodynamic therapy of tumours, J. Photochem. Photobiol. 39 (1997) 1–18.
[4] W.H. Boehncke, A. Ruck, J. Naumann, W. Sterry, R. Kaufmann, Comparison of sensivity towards photodynamic therapy of cutaneous resident and infiltrating cell types in vitro, Lasers Surg. Med. 19 (1996) 451–457.
[5] M. Capella, A.M. Coelho, S. Menezes, Effect of glucose on photodynamic action of methylene blue in *Escherichia coli* cells, Photochem. Photobiol. 64 (1996) 205–210.
[6] S. Menezes, M.A.M. Capella, L.R. Caldas, Photodynamic action of methylene blue: repair and mutation in *Escherichia coli*, J. Photochem. Photobiol. B Biol. 5 (1990) 505–517.
[7] K. Orth, D. Russ, G. Beck, A. Ruck, H.G. Beger, Photochemotherapy of experimental colonic tumours with intra-tumorally applied methylene blue, Langenbeck's Arch. Surg. 383 (1998) 276–281.
[8] K. Miller-Breitkreutz, H. Mohr, Infection cycle of herpes viruses after photodynamic treatment with methylene blue and light, Beitr. Infusionsther. Transfusionsmed. 34 (1997) 37–42.
[9] H. Mohr, B. Bachmann, A. Klein-Struckmeier, B. Lambrecht, Virus inactivation of blood products by phenothiazine dyes and light, Photochem. Photobiol. 65 (1997) 441–445.
[10] K. Orth, A. Ruck, G. Beck, A. Stanescu, H.G. Beger, Photodynamic therapy of small adenocarcinomas with methylene blue, Chirurg 66 (1995) 1254–1257.
[11] K. Orth, A. Ruck, A. Stanescu, H.G. Beger, Intraluminal treatment of inoperable oesophageal tumours by intralesional photodynamic therapy with methylene blue, Lancet 345 (1995) 519–520.
[12] J.D. Spikes, R. Straight, Sensitized photochemical processes in biological systems, Annu. Rev. Phys. Chem. 18 (1967) 409–436.
[13] J.E. Schneider Jr, T. Tabatabaie, L. Maidt, R.H. Smith, X. Nguyen, Q. Pye, R.A. Floyd, Potential mechanisms of photodynamic inactivation of virus by methylene blue, I. RNA-protein crosslinks and other oxidative lesions in Q beta bacteriophage. Photochem. Photobiol. 67 (1998) 350–357.
[14] J.E. Schneider, S. Price, L. Maidt, J.M.C. Gatteridge, R.A. Floyd, Methylene blue plus light mediates 8-hydroxy-2′-deoxyguanosine formation in DNA preferentially over strand breakage, Nucleic Acids Res. 18 (1990) 631–635.
[15] M.M. Gottesman, I. Pastan, Biochemistry of multidrug resistance mediated by the multidrug transporter, Annu. Rev. Biochem. 62 (1993) 385–427.
[16] T. Tsuruo, H. Iida, S. Tsukagoshi, Y. Sakurai, Overcoming of vincristine resistance in P388 leukemia 'in vivo' and 'in vitro' through enhanced cytotoxicity of vincristine and vinblastine by verapamil, Cancer Res. 41 (1981) 1967–1972.
[17] P.R. Twentyman, Cyclosporine as drug resistance modifiers, Biochem. Pharmacol. 43 (1992) 109–117.
[18] A. Ramu, N. Ramu, Reversal of multidrug resistance by phenothiazines and structurally related compounds, Cancer Chemother. 30 (1992) 165–173.

[19] J.M. Ford, W.C. Prozialeck, W.N. Hait, Structural features determining activity of phenothiazines and related drugs for inhibition of cell growth and reversal of multidrug resistance, Mol. Pharmacol. 35 (1989) 105–115.

[20] R.E. Vandoni, J.F. Cuttat, S. Wicky, M. Suter, CT-guided methylene-blue labelling before thoracoscopic resection of pulmonary nodules, Eur. J. Cardio-thorac Surg. 14 (1998) 265–270.

[21] E.M. Link, R.N. Carpenter, G. Hansen, ^{211}At-methylene blue for targeted radiotherapy of human melanoma xenografts: dose fractionation in the treatment of cutaneous tumours, Eur. J. Cancer. 32A (1996) 1240–1247.

[22] R. Yang, X. Yin, X. Zhang, Methylene blue staining in fiber-optic bronchoscopy in the diagnosis of bronchial tumors, Chung Hua. Wai. Ko. Tsa. Chih. 34 (1996) 167–169.

[23] M.A.M. Capella, M. Orind, M.M. Morales, V.M. Rumjanek, Gil Lopes A, Expression of functionally P-glycoprotein in MA104 kidney cells. Z. Naturforsch. 54 (1999) 119–127.

[24] M. Horio, I. Pastan, M.M. Gottesman, J.S. Handler, Transepithelial transport of vinblastine by kidney-derived cell lines, Application of a new kinetic model to estimate in situ K_m of the pump. Biochim. Biophys. Acta 1027 (1990) 116–122.

[25] T. Tsuruo, H. Iida, E. Ohkochi, S. Tsukagoshi, Y. Sakurai, Establishment and properties of a vincristine-resistant human myelogenous leukemia K562, Jpn. J. Cancer Res. 74 (1983) 751–758.

[26] M.A.M. Capella, L.S. Capella, J.S.M. Alcantara, V. Moura-Neto, A.G. Lopes, Vanadate is toxic to adherent-growing multidrug resistant cells, Tumor Biol. 21 (2000) 54–62.

[27] H. Takeshita, K. Kusuzaki, T. Ashihara, M.C. Gebhardt, H.J. Mankin, Y. Hirasawa, Actin organization associated with the expression of multidrug resistant phenotype in osteosarcoma cells and the effect of actin depolymerization on drug resistance, Cancer Lett. 126 (1998) 75–81.

[28] A.A. Neyfakh, Use of fluorescent dyes as molecular probes for the studies of multidrug resistance, Exp. Cell Res. 174 (1988) 168–176.

[29] V.M. Rumjanek, M. Lucena, M.M. Campos, V.M. Marques-Silva, R.C. Maia, Multidrug resistance in leukaemias: the problem and some approaches to its circumvention, Cienc. Cult. 46 (1994) 63–69.

[30] M.A.M. Capella, S. Menezes, Synergism between electrolysis and methylene blue photodynamic action in *Escherichia coli*, Int. J. Radiat. Biol. 62 (1992) 321–326.

[31] J.H. Zar, Biostatistical Analysis, 3rd Edition, Prentice-Hall, Englewood Cliffs, NJ, 1996, pp. 211–233.

[32] M. Dellinger, G. Moreno, C. Salet, H. Tapiero, T.J. Lampidis, Cytotoxic and photodynamic effects of Photofrin on sensitive and multi-drug-resistant Friend leukaemia cells, Int. J. Radiat. Biol. 62 (1992) 735–741.

[33] S.F. Purkiss, M.F. Grahn, M. Turkish, M.G. Macey, N.S. Williams, In vitro modulation of haematoporphyrin derivative photodynamic therapy on colorectal carcinoma multicellular spheroids by verapamil, Br. J. Surg. 79 (1992) 120–125.

[34] E. Schick, R. Kaufmann, A. Rück, A. Hainzl, W.-H. Boehncke, Influence of activation and differentiation of cells on the effectiveness of photodynamic therapy, Acta Derm. Venereol. 75 (1995) 276–279.

[35] Y.S. Lee, R.D. Wurster, Methylene blue induces cytotoxicity in human brain tumor cells, Cancer Lett. 88 (1995) 141–145.